Paleointensity of the earth's magnetic late quaternary volcanic sequences at (Indian ocean) field recorded by the island of La Réunion

Annick Chauvin, Pierre-Yves Gillot, Norbert Bonhommet

JOURNAL OF GEOPHYSICAL RESEARCH, VOL. 96, NO. B2, PAGES 1981–2006, FEBRUARY 10, 1991

Paleointensity of the Earth's Magnetic Field Recorded by Two Late Quaternary Volcanic Sequences at the Island of La Réunion (Indian Ocean)

ANNICK CHAUVIN

Laboratoire de Géophysique Interne, CAESS, Université de Rennes I, France

PIERRE-YVES GILLOT

Centre des Faibles Radioactivités, CEA-CNRS, Gif/Yvette, France

NORBERT BONHOMMET[1]

Laboratoire de Géophysique Interne, CAESS, Université de Rennes I, France

A paleomagnetic study has been undertaken on two late Quaternary volcanic sequences from the Piton de la Fournaise volcano (island of La Réunion) in order to provide absolute paleointensities of the Earth's magnetic field from a site in the southern hemisphere. The pattern of secular variation recorded by both sequences clearly indicates that the extrusion rate of the lava flows was not constant with time. A detailed investigation of the magnetic properties of the samples was carried out in parallel with paleointensity experiments which were performed with the Thellier method. Samples with minimum overprint, composed by single-domain or pseudo-single-domain magnetite showing good thermal stability and a narrow blocking temperature spectrum were the most successful during Thellier's experiments. Values of the paleofield strength from 19 to 55 mT have been obtained on 23 flows among the 30 which were sampled. Few variations (7.5-9.9 x 10^{22} A m^2) are observed in the virtual dipole moments (VDMs) determined on the youngest sequence (5-12 ka). Those values are within the range of fluctuations of the worldwide variations of VDMs for this period. On the other hand, data from the oldest sequence (82-98 ka) are the first paleointensity values obtained in that time period, and the observed VDMs extend from 4.1 to 8.8 x 10^{22} A m^2. These results suggest that for this time interval, the field did not depart from its average behavior.

INTRODUCTION

Late Quaternary secular variations of the Earth's magnetic field are recorded by different materials, archaeological artifacts, dated lava flows, and lake or marine sediments. The direction of the past geomagnetic field is generally easily determined because it is almost equal to the direction of the magnetic remanence. In contrast, the intensity of the magnetic remanence is not only dependent on the intensity of the field but also is strongly related to the material, thus making the determination of the paleointensity of the geomagnetic field more difficult to establish than its paleodirection. Although the knowledge of the variations of intensity of the geomagnetic field is as important as its directional behavior, very few studies describe the paleomagnetic field as a complete vector.

Volcanic rocks as well as archaeological materials provide spot readings of the geomagnetic field, while sediments provide the only means of obtaining continuous records of the secular variation at one site. Moreover, sedimentary records from lake or marine cores are numerous enough to allow a better geographic coverage. However, the magnetization process is complex and supposed to smooth the original magnetic signal. Another major drawback to sediments is the difficulty in recovering the paleointensity from the paleomagnetic record. In the best cases, only relative paleointensity changes can be obtained [*Levi and Banerjee*, 1976; *King et al.*, 1983]. Thermoremanent magnetizations (TRM) of volcanic deposits and archaeological materials allow the determinations of both direction and absolute intensity of the geomagnetic

1 Now at Département de Géotectonique, Université de Paris VI, France.

Paper number 90JB02223.
0148-0227/91/90JB-02223$05.00

field, because TRM is proportional to the weak inducing field and can be reproduced in the laboratory.

Paleointensity data for the late Quaternary have been mostly obtained from the northern hemisphere, Europe [*Schweitzer and Soffel*, 1980; *Kovacheva*, 1980, 1983; *Thellier and Thellier*, 1959; *Salis*, 1987; 1989, *Burlatskaya*, 1983; *Walton*, 1979, 1984; *Aitken et al.*, 1984], Egypt [*Games*, 1980, 1983a; *Aitken et al.*, 1983], India [*Ramaswamy et al.*, 1985], Japan [*Tanaka*, 1980 ; *Hirooka*, 1983], Hawaii [*Coe*, 1967a; *Coe et al.*, 1978], China [*Wei et al.*, 1987], and North America [*Sternberg and Butler*, 1978; *Sternberg*, 1983, 1989; *Champion*, 1980]. Only few data from Australia [*Barbetti*, 1983] and Peru [*Kono et al.*, 1986; *Games*, 1983b] constitute the data base for the southern hemisphere. Moreover, most of these data correspond to the last 2000 years. Paleointensity data indicate that the strength of the paleofield at any locality can change by a factor of 2 over a period of time as short as a few hundred years [*Kovacheva*, 1982; *Barbetti*, 1983]. Such variations in intensity associated with uncertainties in the age determinations and the poor geographic distribution of the sites make the analysis of global intensity data difficult [*Merrill and McElhinny*, 1983].

Compilations of worldwide paleointensity data have been performed for three periods of time, the last 12,000 years, the last 50,000 years, and the last 5 m.y. [*Barton et al.*, 1979; *McElhinny and Senanayake*, 1982; *McFadden and McElhinny*, 1982]. By averaging the field over short periods of a few hundreds years (500 or 1000 years) and for several localities, the nondipole contribution is assumed to be averaged out. In this way, a curve of the variations of the mean virtual dipole moments versus time was established for the last 10,000 years. In the time interval 15,000-50,000 there is some strong evidence that the field was lower than in more recent time [*McElhinny and Senanayake*, 1982; *Salis*, 1987], as well as compared with the average field for the last 5 m.y. Also, a detailed statistical analysis of the VDMs for the last 5 m.y. indicates that nondipole fields are almost proportional to the strength of the dipole field [*McFadden and McElhinny*, 1982].

In this paper, we will report a detailed paleomagnetic study of two young volcanic sequences from the island of La Réunion (Indian Ocean, 21°S). Several paleointensity determinations have been attempted using the *Thellier and Thellier* [1959] stepwise double heating method which has been considered as the most reliable [*Coe and Gromme*, 1973; *Prévot et al.*, 1985; *Aitken et al.*, 1988].

GEOLOGY GEOCHRONOLOGY AND SAMPLING

The island of La Réunion lies in the western Indian Ocean (21°S, 55.5°E°). It belongs, with Mauritius and the Mascarene Plateau trend, to a volcanic lineament linked to a hot spot the present position of which would be 170 km west of Réunion [*Emerick and Duncan*, 1982]. It is constituted of two shield volcanoes (Figure 1). The larger one, the Piton des Neiges which occupies the northwestern part of the island, is now extinct, while the youngest, the Piton de la Fournaise, is still active. The first stratigraphy and chronology of the volcanics, based on K-Ar radiometric age determinations, were established by *McDougall* [1971]. The addition of more recent studies [*Gillot and Nativel*, 1982; *Gillot and Nativel*, 1989] helped define the geological evolution of the island. The Piton des Neiges edifice is composed of two different series of lavas: an oceanitic and a

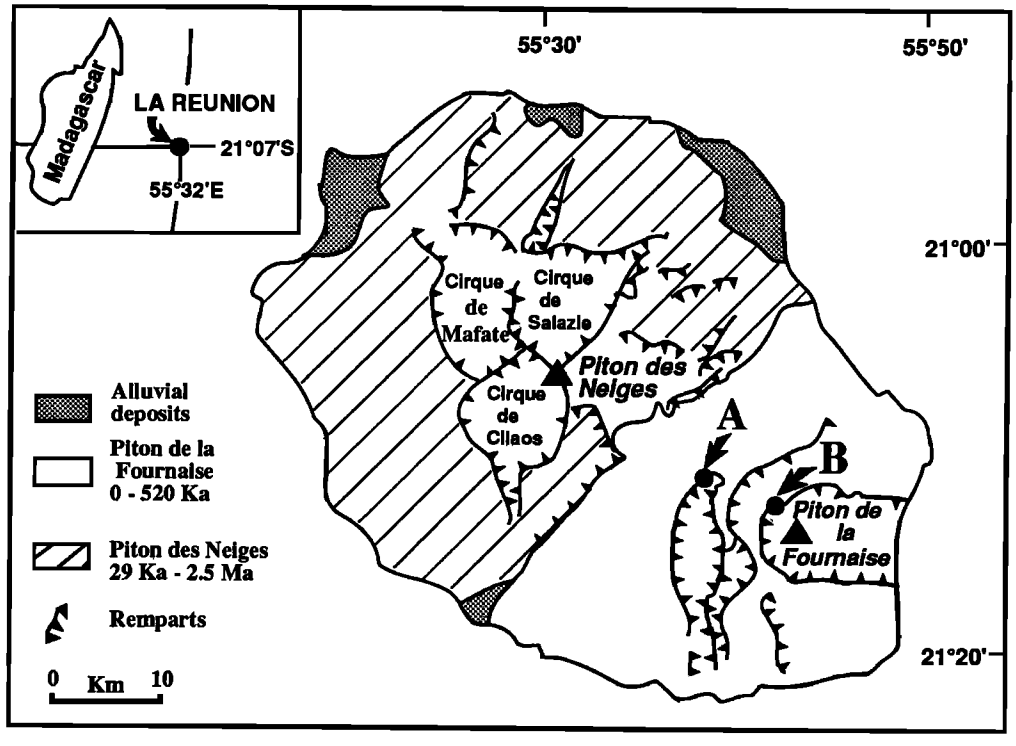

Fig. 1. Sampling map of the island of La Réunion showing the two volcanos (Piton des Neiges and Piton de la Fournaise). The sampling corresponds to two vertical sections at site A and B.

differentiated series. The oceanitic units extend from 2 to 0.4 Ma. The activity of the Piton de la Fournaise started at the time of the last extrusions of the oceanite formation at the Piton des Neiges (between 0.53 and 0.43 Ma) and developed essentially while Piton des Neiges differentiated products were erupted ; the activity of Piton des Neiges ended around 30 ka. Four volcanic phases are recognized at the Piton de la Fournaise separated by huge successive gravity slumps [*Duffield et al.*, 1982] which developed U-shaped calderas open on the eastern or seaward side; the products of the successive phases in turn filled up these calderas. The first phase, the older products of which are from 0.53 Ma, finished around 0.28 Ma with the collapse of the caldera corresponding to the Rivière de Remparts western wall. The second cycle extends between 0.22 and 0.06 Ma. It is marked by the collapse of the second caldera, the Rempart des Sables. The products of the third phase are not deeply cut by erosion; it is thus impossible to date its beginning. It finished around 4.7 Ka [*Bachelery*, 1981] with the Rempart de Bellecombe caldera collapse, delimiting the Enclos Fouqué in which were erupted the products of the fourth phase and where the present volcanic activity is located and linked to the two active Bory and Dolomieu craters.

The age determination of very young volcanic rocks by the K-Ar method is difficult because of the slow decay constant of ^{40}K. Argon is also a major component of the atmosphere and equilibrates with the lavas as they cool. Thus, attention must be paid to the principal correction in age calculation, that for atmosphere argon contamination. Several factors may limit the precise measurement of small amounts of radiogenic ^{40}Ar within a total Ar signal, which is composed principally of atmospheric argon trapped by the sample and the extraction system. The technique of *Cassignol and Gillot* [1982] reduces, as far as possible, the uncertainties in the argon measurement on the basis of a double comparison of the sample argon and atmospheric argon under rigorously identical analytical conditions. It involves the accurate estimation of the departure of the sample $^{40}Ar/^{36}Ar$ ratio from the atmospheric one and thus the measurement of very low radiogenic ^{40}Ar percentages (down to 0.12%). The technique makes it possible to insure an absolute calibration of the signal of total ^{40}Ar, omiting the spike of ^{38}Ar and the uncertainties linked to it. Samples dated by the Centre des Faibles Radioactivités were collected during the same field trip as those used for paleomagnetic study. K-Ar ages are given at the $\pm 2\sigma$ level.

Two volcanic sections from the Piton de la Fournaise were sampled (see Figure 1). The first section called Remparts de Bellecombe (site B) consists of 13 lava flows and represents a stratigraphic height of 100 m in the products of the third phase exposed along the caldera wall. The top of this section has been dated by ^{14}C performed on carbonized wood [*Bachelery*, 1981] at 4754 years and the eighth flow gives a K-Ar age of 11 ka ± 2.6. Seventeen lava flows constitute the second section called Rivière des Remparts (site A) with an approximative thickness of 185 m. Radiometric age determinations by K-Ar have given ages of 82 ka ± 6.0 for the first lava, 85.5 ka ± 3.0 for the sixth and 98 ka. ± 4.0 for the last lava flow sampled, at the bottom of the section. One hundred seventy-seven cores were collected, using a gasoline-powered portable core drill and oriented with Sun and magnetic compass. This gives an average of five to six cores per flow.

REMANENT DIRECTIONS

Measurements and demagnetizations were carried out using a Schonstedt magnetometer and demagnetizer. Natural remanent magnetization (NRM) intensity ranges from 1 to 40 A m^{-1}, with a maximum in the distribution around 7-10 A m^{-1} (Figure 2).

Stepwise thermal or alternating field (AF) demagnetizations were performed on one specimen from each core. Characteristic directions were obtained according to the best fitting line on orthogonal vector plots. In computing the mean directions for each flow, a few samples were omitted if field notes suggested possible orientation mistakes or if complete cleaning of the secondary magnetization was not obtained, especially in the case of strong magnetic overprint due to lightning recorded by two flows at site A (RA10 and RA12). The variations in the shape of the AF demagnetization curves are as important within different flows as within samples from a same flow. About 30% of samples from the site A have medium demagnetizing fields (MDF) higher or equal to 30 mT, while almost

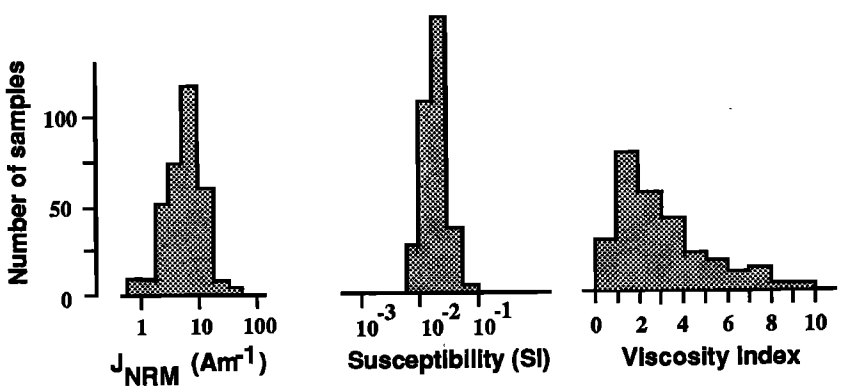

Fig. 2. Distribution of the intensity of remanent magnetization (J_{NRM}), weak field susceptibility (SI) and viscosity index for all specimens.

three-quarters of samples from the site B have this high stability against AF. The wide spectrum of unblocking temperatures indicates that titanomagnetites are the magnetic carriers of the remanence.

Results From Site B: Rempart de Bellecombe (Table 1 and Figure 3)

The mean directions per flow are listed in Table 1 and plotted on a stereographic projection (Figure 3). According to the radiometric age determinations, this section represents a time interval of few thousands years but less than 10 ka. From Figure 3, two groups of directions can easily be identified (RB1-RB9 and RB10-RB12). On the other hand, the first group from RB1 to RB9 has an elongated pattern which can be subdivided into three small groups of successive flows having recorded very close directions (RB9-RB5, RB4-RB3, and RB2-RB1) (see also Table 1). The low number of samples (five to six) per flow does not enable statistical distinction using α_{95}. The precision parameter of Fisher statistics associated with the mean direction (0°.0, -43°) calculated for all the 13 units is relatively high (k=105) and confirms that a small part of secular variation was recorded at this site.

Results From Site A: Rivière des Remparts (Table 1 and Figure 3)

The distribution of the paleomagnetic directions shows greater variations than those observed in the previous sequence. Although the low number of samples per flow makes statistical tests inconclusive, several groups of successive flows having recorded similar

TABLE 1 Paleomagnetic data

Lava Flows	*n/N*	*D*	*I*	*k*	α_{95}	Lat deg	long deg	J_{NRM}	χ
				Rivière des Remparts: Site A					
RA1	3/5	7.8	-45.2	68.3	15.0	81.0	184.8	15.5	2.3
RA2	3/5	1.5	-48.5	249.2	7.8	81.6	226.5	6.7	2.2
RA3	3/8	1.3	-43.4	116.0	11.5	85.7	219.5	8.4	1.6
RA4	4/5	352.0	-64.8	135.6	7.9	63.6	247.9	2.4	1.3
RA5	3/5	353.1	-63.9	25.0	25.2	65.0	247.0	3.5	1.3
RA6	3/6	343.7	-61.0	220.3	8.3	65.1	265.1	3.7	1.3
RA7	6/6	350.9	-57.8	202.8	4.7	71.1	257.9	2.6	2.0
RA8	6/6	346.4	-58.8	97.5	6.8	68.3	264.8	2.1	3.3
RA9	5/6	348.8	-58.1	358.2	4.0	70.0	261.7	2.4	3.0
RA10	4/6	5.6	-47.9	17.5	22.6	80.7	203.5	13.0	2.2
RA11	6/8	3.4	-52.6	161.1	5.3	77.6	222.1	2.7	1.1
RA12	2/6	332.9	-39.0	-	-	64.8	318.5	5.8	1.1
RA13	5/5	335.9	-43.9	549.2	3.3	67.5	309.3	4.7	2.9
RA14	6/6	334.3	-50.5	139.9	5.7	64.9	296.6	1.0	2.4
RA15	6/6	335.1	-38.4	158.9	5.3	66.8	319.9	5.2	2.2
RA16	6/7	359.1	-36.7	112.3	6.3	88.9	7.4	5.6	3.0
RA17	6/7	351.9	-44.0	194.2	4.8	81.3	292.3	3.2	3.5
Mean	17	350.7	-50.9	46.7	5.3	76.2	269.8		
				Remparts de Bellecombe: Site B					
RB1	6/6	1.1	-40.9	208.6	4.6	87.6	211.1	9.8	1.3
RB2	5/6	0.8	-41.4	150.5	6.3	87.3	219.7	8.6	1.5
RB3	5/5	358.7	-33.2	139.8	6.5	86.7	33.6	8.9	1.5
RB3bis	5/5	357.9	-38.4	918.7	2.5	88.0	313.0	9.7	1.5
RB4	6/6	356.0	-34.8	406.6	3.3	85.7	353.3	6.7	1.6
RB5	5/5	3.8	-41.0	461.2	3.6	86.3	184.7	7.7	1.4
RB6	6/6	5.4	-43.8	129.5	5.9	83.4	188.3	5.4	1.6
RB7	5/7	10.6	-41.8	579.0	3.2	79.8	163.9	5.3	2.2
RB8	5/5	6.7	-43.8	87.8	8.2	82.4	182.5	8.0	1.8
RB9	5/5	4.7	-42.5	73.0	9.0	84.5	184.7	7.5	0.9
RB10	5/5	350.0	-50.0	117.8	5.8	76.9	276.5	9.6	2.4
RB11	5/5	352.6	-53.5	262.7	4.7	75.6	260.9	8.5	1.6
RB12	5/5	347.7	-54.3	140.6	6.5	72.6	271.3	9.2	3.5
Mean	13	0.0	-43.2	104.7	4.1	85.7	237.9		

RA (Réunion site A); RB (Réunion site B). *n/N*: number of samples used in the calculation/total number of samples collected; *D*, *I*, mean declination and inclination; *k*, precision parameter of Fisher; α_{95}, 95% confidence cone about mean direction; Lat, Long: latitude and longitude of the VGPs; J_{NRM}, geometric mean NRM intensity; χ, geometric mean susceptibility (SI units).

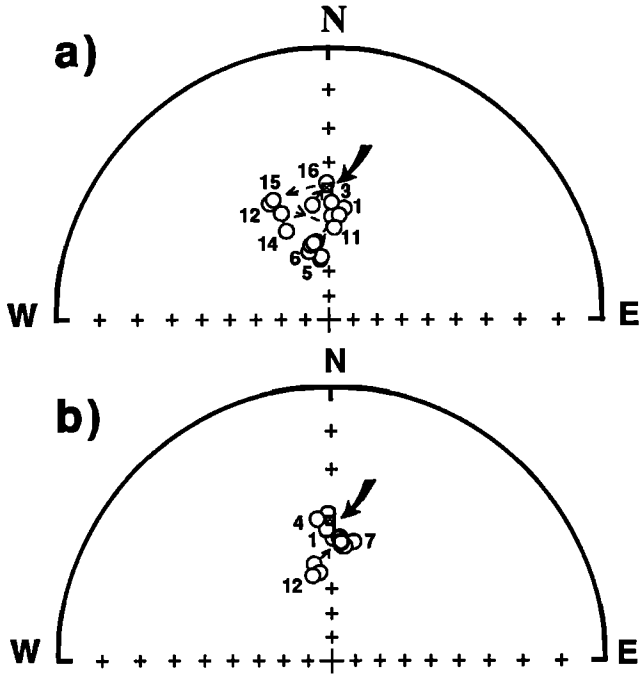

Fig. 3. Stereographic projection of mean paleomagnetic directions per flow for both sequences: (a) site A, (b) site B. Open circles are projection on the upper hemisphere. The sequences of flows are numbered from top to bottom; the squares pointed out by the arrows correspond to the geocentric axial dipole direction.

directions may be identified on the stereographic projection (Figure 3). For example, the first flows RA1-RA3 have close directions with an inclination of about -45°, while the underlying flows (RA4-RA9) have steep inclinations of about -60°. Flows RA10 and RA11 have similar directions than the first group, on the top of the section. The underlying group of flows (RA15 -RA12) have northwest declinations. At the bottom of the section, the two flows RA17 and RA16 have recorded directions close to the axial dipole direction expected at this site.

Almost all individual directions have steeper inclinations than the one expected from an axial dipole. The mean VGP for the section is at more than 10° from the geographic axis. The total angular dispersion of VGPs (ST), if we discard flow RA12 for which only two samples were used in computing the mean direction, has a value of 12.5. The angular dispersion of the field (SF= 11.7) has lower and upper limits [*Cox*, 1969] at 95% of 9.3 and 15.6 (with $SF^2=ST^2-SW^2/n$, SW is the average angular dispersion within flows, here SW=9.6 and n is the average number of samples per flow; here n=4.7). This value of angular dispersion is lower than the one given by recent models of secular variation, for example models, F and G of *McFadden and Merrill* [1984] and *McFadden et al.* [1988], but is within the statistical confidence limits. However, this computation was performed with a small number of flows, and errors bars are quite large (9.3-15.6). Moreover the Fisher parameter dispersion is about twice the value expected for a site at this latitude. So we believe that this test is inconclusive and the departure of the mean VGP from geographic axis is then interpreted as the result of a partial sampling of secular variation path. Comparison with previous studies, based on better geographically distributed sampling, at La Réunion [*Watkins*, 1973; *Chamalaun*, 1968] or at other islands in the Indian Ocean [*Watkins and Nougier*, 1973] clearly indicates that our sampling at site A did not record a similar amount of variation of the magnetic field.

According to the radiometric datings, both sections A and B cover a time interval of a few thousands years. A question arises: Have the flows been extruded regularly over these time intervals? Radiometric methods are unable to resolve such fine scale variations. In contrast, the pattern of paleosecular variation may be used to constrain the chronology of past volcanic activity. It is very likely that jumps in the secular variation record would correspond to hiatus in the volcanic activity, and paleomagnetism enables identification of these gaps but does not put any constraint on their length. Several jumps are observed at the site Rivière des Remparts (RA3-RA4; RA9-RA10; RA11-RA12; RA15-RA16) (see Figure 3 and Table 1). In contrast, only one major discontinuity (RB9-RB10) is apparent at Remparts de Bellecombe. We will see later that variations in paleointensities fit the directional behavior quite well.

MAGNETIC PROPERTIES

The investigation of the magnetic properties of our samples has been conducted for a better understanding of the behavior of the samples during paleointensity experiments. Measurements of weak field susceptibility at room temperature and of the viscosity index, strong field thermomagnetic experiments, and records of variations of weak field susceptibility from liquid nitrogen to room temperature were performed for almost all cores. Saturation magnetization J_S and saturation remanence J_{TS} were determined for about 40 samples from the two sampled sites. Lowrie-Fuller tests [*Lowrie and Fuller*, 1971], which consist of comparing the shape of AF demagnetization curves of the natural remanent magnetization (NRM) with curves of isothermal remanent magnetization (IRM) acquisition, are also available for these samples.

Weak Field Susceptibility at Room Temperature

Weak field susceptibility at room temperature was determined using a Bartington susceptibility meter. Susceptibility values typically range from 10^{-2} to 7.5 x 10^{-2} SI units (see Figure 2).

Magnetic Viscosity

The distribution of viscosity indexes, which are the ratio of the intensity of the viscous remanent magnetization (VRM) acquired within 10 days of storage in the laboratory field to that of the NRM [*Thellier and Thellier*, 1944], is shown in Figure 2. This test was performed on all specimens (299). Most of the samples (80%) have a viscosity index lower than 5%.

Thermomagnetic Behavior

Strong field thermomagnetic (J_S-T) experiments using an automated Curie balance, with heating and cooling rate of 8°C/minute, were done in vacuum in order to minimize oxidation during heating. These experiments provide information on the samples magnetic phases (Curie point) and magnetochemical changes during heating. In order to better define temperatures at which such magnetochemical changes occurred, the heating runs were commonly interrupted three times, allowing the sample to cool about 50°C after which heating was resumed.

Among the three methods generally used to determine the Curie temperatures of rocks [*Gromme et al.*, 1969; *Moskowitz*, 1981; *Prévot et al.*, 1983], the one corresponding to the temperature of the inflection point of the thermomagnetic curve was chosen, because it provides a better estimate of the broad distribution of Curie points within such rocks [*Prévot et al.*, 1983].

Thermomagnetic experiments were performed on 165 samples. Two Curie points were often determined for an individual sample. Variations in magnetic mineralogy occur between different samples of the same lava flow as well as between flows. Only samples from flows RA4, RA5, and RA6 have predominant low Curie temperatures. The reversibility of the heating and cooling curves shows evidence of stoichiometry; indeed low temperature oxidation produces cation-deficient titanomagnetites for which thermomagnetic curves are not reversible.

Thermomagnetic experiments provide quantitative values of the Curie points, but the information associated with mineralogical changes between heating and cooling is much more difficult to quantify. For this reason, the various J_S-T curves have been grouped into four different categories (Figure 4) which will be described in detail. However, we must say that such classifications are not always clearly delimited because there is a continuous spectrum of variations between samples, rather than sharp distinctions.

The most common encountered type (type 1 curves, 87 samples) shows a single Curie point ranging from 480° to 560°C. It can be subdivided into five categories according to the shape of the cooling curves, changes in Curie temperature and J_S intensity after heating at about 600°C. Curves of type 1a (20 samples) show a single well-defined Curie point and little changes between heating and cooling curves. Decrease in J_S, after heating is less than 4%. The change in J_S for type 1b (28 samples) curves is less than 10% at room temperatures, but heating and cooling curves differ in shape for temperatures above 200°C, and the Curie point during cooling is always lower by a few degrees than during heating. Type 1c curves correspond to 16 samples for which the cooling curves crosse the heating curves at temperature between 150° to 300°C. For this group, an increase in J_S is observed after heating (from 5 to 12%) and Curie temperatures decrease by a few degrees. Type 1d curves (seven samples) exhibit a large increase in J_S (up to 28%) at temperatures between 400° and 500°C, while no change in Curie temperatures is observed after

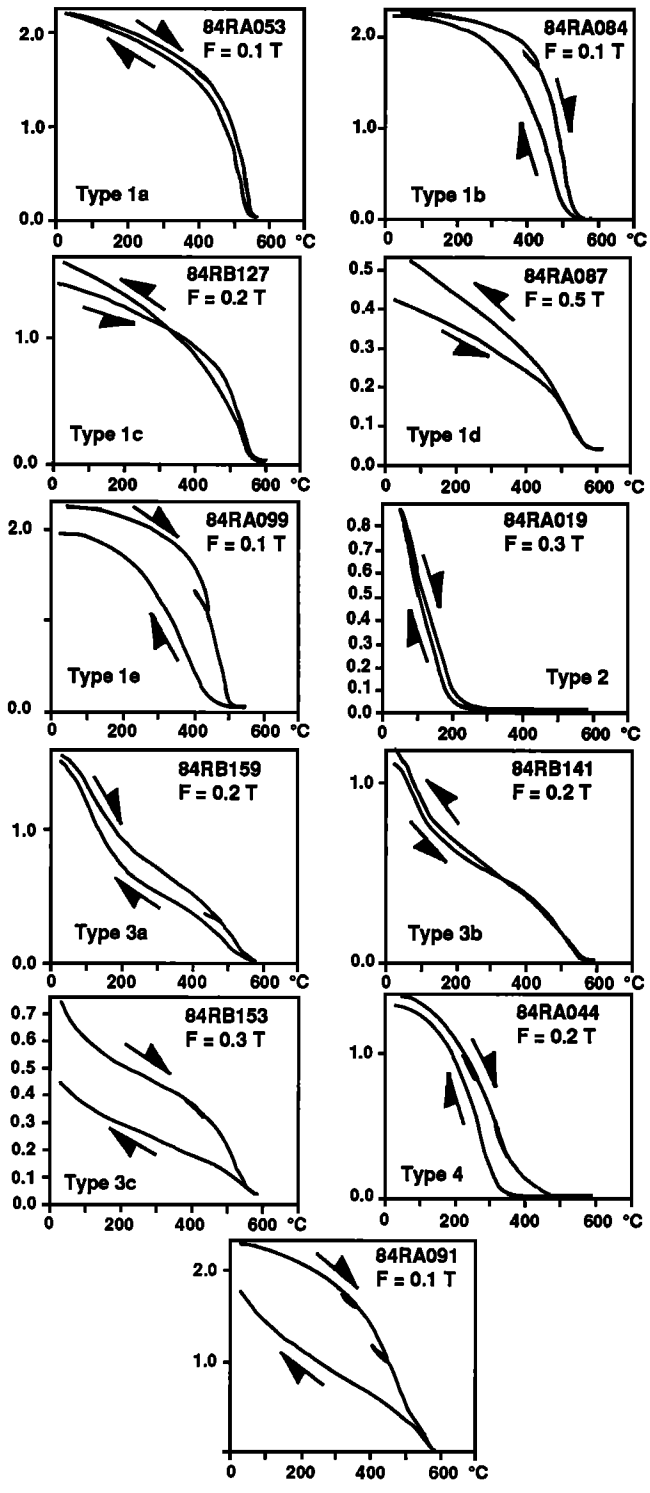

Fig. 4. Examples of Curie experiments performed in vacuum showing the different types of behavior. The value of the applied field (F, in tesla) is indicated for each experiment. Heating and cooling curves are shown by arrows. The unit of the magnetic moment (J_S) is given in A m^2 Kg^{-1}

cooling. Finally, type 1e curves (11 samples) correspond to irreversible heating and cooling curves. A decrease in J_S of more than 10% and a reduction of the Curie temperature by a few tens of degrees are also observed. The magnetic phases which produce type 1 curves could

be either an original Ti-poor titanomagnetite or more probably be a result of high-temperature oxidation of a primary Ti-rich titanomagnetite to a Ti-poor titanomagnetite containing ilmenite lamellae, in agreement with our optical microscope observations.

Type 2 curves (nine samples) show a single ferrimagnetic phase with Curie temperature below 200°C and a good reversibility of the heating and cooling curves. According to the reversibility of the curves during the experiment, we can expect that these Ti-rich titanomagnetites were not oxidized at low temperature; that is the oxidation index z is very small (about 0). Using a contour diagram given by *Readman and O'Reilly* [1972], Curie points lower than 200°C would indicate a titanium content parameter x around 0.7 to 0.6. Titanomagnetites with such x values are often observed on mid-ocean ridge basalts [*Prévot et al.*, 1983; *Gromme et al.*, 1979].

Type 3 curves are characterized by the presence of two ferrimagnetic phases. The first one has Curie temperatures between room temperature and 300°C, the second has higher Curie points commonly ranging from 480° to 550°C. These types of curves were produced by 66 samples. Depending on whether or not the cooling curve rewords the heating cycle, three categories can be defined in this group. Type 3a curves (36 samples) show little change in J_S after cooling, while the two Curie points are not altered. The cooling and heating curves for the 13 samples which compose type 3b cross at temperatures between 200° and 300°C. Type 3c curves show an irreversible change in the magnetic phase after heating, and J_S is greatly reduced (15-50%). These bimodal curves are often observed on samples where high-temperature deuteric oxidation has not been completed, converting only one part of a primary high Ti titanomagnetite to a Ti-poor titanomagnetite [*Ade-Hall et al.*, 1971]. Irreversibility of the heating and cooling curves is interpreted as reflecting some low-temperature oxidation of one (or both) magnetic phase.

Type 4 thermomagnetic curves are represented by only three samples from the same flow, showing an unusual single Curie point between 300° and 430°C.

Irregularities in the common uniform decrease in J_S, at the end of the heating cycles have been noted on some curves of types 3 and 1 (sample RA091, Figure 4). They seem similar to those pointed out by *Mankinen et al.* [1985]. According to Mankinen et al.these authors we attribute these features to the presence of two different Ti-poor titanomagnetites.

Low Temperature Behavior of Weak Field Susceptibility χ

Several workers [*Radhakrishnamurty and Deutsch*, 1974; *Radhakrishnamurty et al.*, 1979; *Senanayake and McElhinny*, 1981, 1982] have studied the variation in magnetic susceptibility of basalts from liquid nitrogen temperature (78°K) to room temperature.

Senanayake and McElhinny [1981] have shown that according to their low-temperature characteristics, more than 95% of their basalts could be classified into three groups (Figure 5). Group 1 samples show a decay in

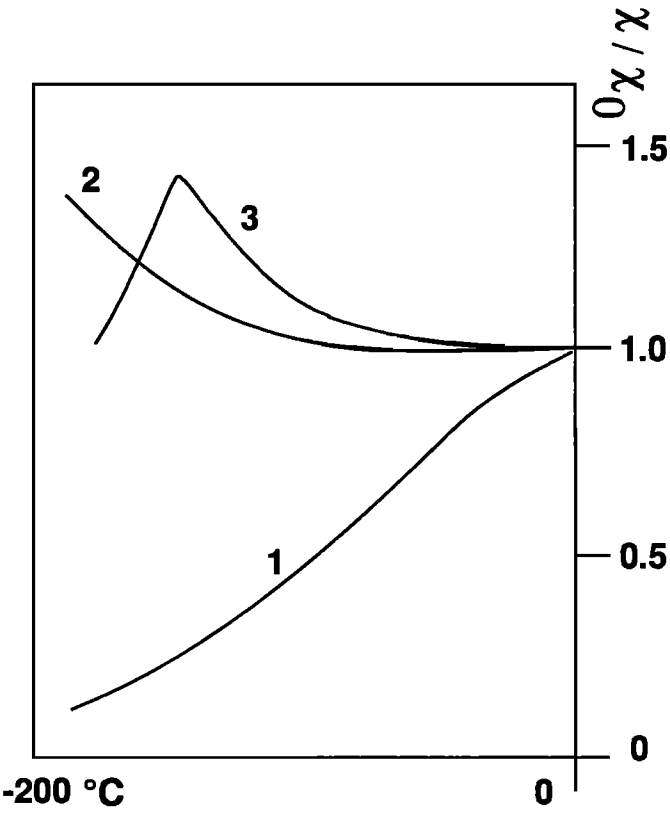

Fig. 5. Behavior of the weak field susceptibility from nitrogen temperature to room temperature (χ-T curves). Following *Senanayake and McElhinny* [1982], type 1 curves may correspond to Ti-rich titanomagnetites predominantly MD, type 2 curves to Ti-poor titanomagnetites with many ilmenite lamellae, and type 3 to multidomain magnetites.

susceptibility to an average value of 0.28 of the room temperature value, at 78°K. Group 2 samples exhibit an increase in susceptibility to an average value of 1.26 of the room temperature value at 78°K. Group 3 samples describe a peak in susceptibility on cooling, averaging 1.24 of the room temperature value, returning to close to the initial value again at 78°K. By comparing these behaviors obtained on natural rock with variation in weak field susceptibility observed on synthetic samples, they concluded that group 1 basalts are dominated by unoxidized titanomagnetites ($x > 0.3$), predominantly multidomain (MD), group 2 samples are mainly titanomagnetite grains with exsolved ilmenite lamellae, while group 3 basalts consists predominantly of multidomain magnetite or Ti-poor titanomagnetite. Because in large grains of Ti-poor titanomagnetite the susceptibility is controlled by magnetocrystalline anisotropy, the susceptibility peak observed in group 3 samples is attributed to the isotropic point, when the sign of the magnetocrystalline constant K_1 changes from negative to positive, around 130°K (i.e., -143°C). Characteristics of group 2 samples were explained by stress effects from the ilmenite lamellae [*Senanayake and McElhinny*, 1981].

Senanayake and McElhinny [1982] then examined the effect of successive heatings on the low-temperature susceptibility of samples from each group. They have

found, after repeating heatings, that group 1 basalts gradually oxidize above 300°C to produce the characteristics of group 2 basalts. This oxidation takes the form of producing exsolved ilmenite lamellae [*Kono*, 1987]. In contrast, both group 2 and group 3 basalts appear stable to oxidation until at least 500°C. Because chemical changes of the magnetic mineralogy are the most limiting factors in paleointensity experiments, they concluded that samples from groups 2 and 3 are the most suitable material for paleointensity.

Given that *Senanayake et al.* [1982] did obtain reliable paleointensity data, using samples selected following this criterium, susceptibility characteristics down to liquid nitrogen temperature have been investigated for most of the Réunion samples.

Low-temperature susceptibility measurements are made in the following way. Both the sample and the thermocouple (Copper-Constantan) are molded using plasticine and are cooled by immersion in liquid nitrogen. Recording of the magnetic susceptibility is performed by a Bartington sensor protected from temperature changes by a water jacket. This prevents any drift of the Bartington susceptibility meter with temperature. Measurements of the susceptibility and the temperature during the warming up of samples are recorded by computer for further numerical analysis and graphical display.

We will now compare the results of these weak field susceptibility low-temperature experiments (i.e., χ-T curves) with some other magnetic parameters in order to differentiate composition and grain size effects.

Comparison with high field thermomagnetic experiments. Some examples of these experiments (Figure 6) are presented in the four different groups according to their Curie points. Samples with Curie temperature below 200 °C all belong to group 1 as defined by *Senanayake and McElhinny* [1981], the value of the susceptibility at liquid nitrogen temperature being one half of that at room temperature. Samples having Curie points higher than 500°C (type 1 of J_S-T curves) can be classified in group 2 or 3, and most of them exhibit the susceptibility peak characteristic of the magnetite magnetocrystalline transition. A few of them show a progressive increase of their susceptibility from liquid nitrogen temperature to room temperature, but the ratio of the low-temperature susceptibility to that at room temperature is greater than 0.65. In fact, such samples have a behavior in between groups 1 and 2 because low-temperature susceptibility behavior is strongly dependent upon the titanium content of the titanomagnetite. This intermediate behavior between groups 1 and 2 is clearly observed for samples having two Curie points or those with a single Curie point between 400° and 500°C.

Comparison with J_{rs}/J_s ratios and remanence coercivities. We have shown a strong correlation between χ-T type curves and Curie points of samples. In order to see if a clear relation exists between χ-T type curves and the domain structure of grains, we have determined the ratio of saturation remanence (J_{rs}) to the saturation magnetization (J_s) for 36 selected samples,

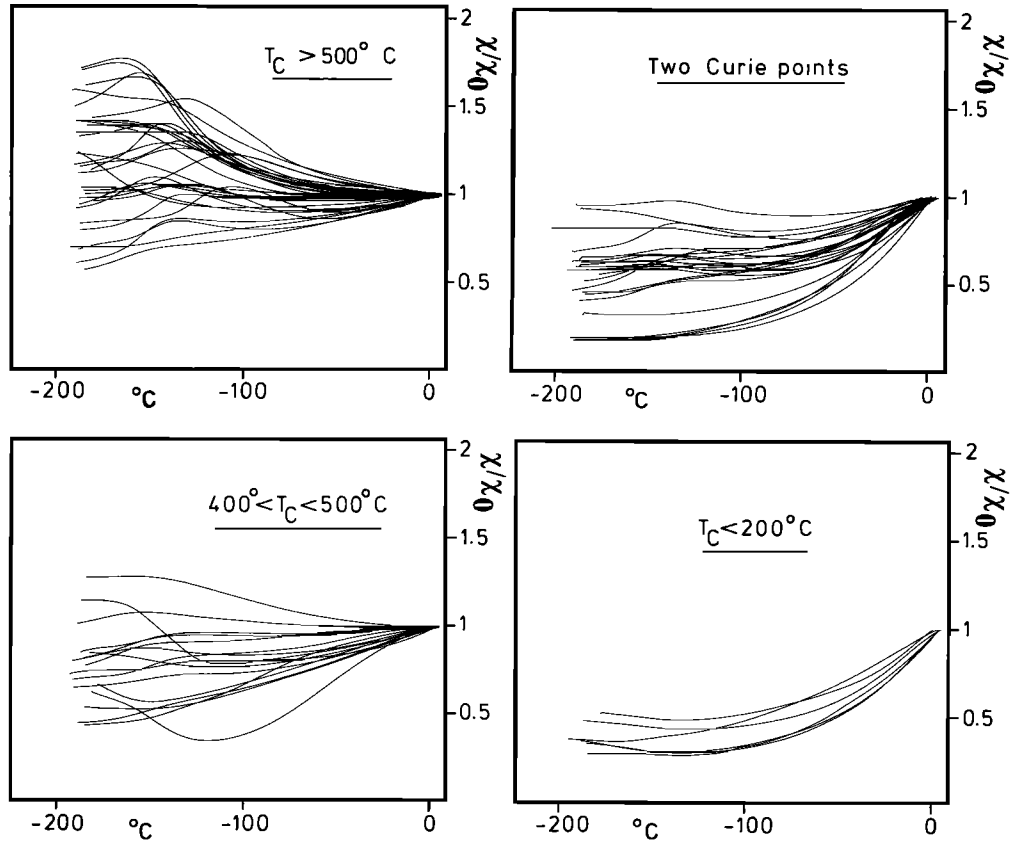

Fig. 6. Correlation between χ-T curves and four groups of Curie points.

which show no significant overprints and which have typical low-temperature susceptibility behavior. This ratio is a good grain size parameter, even if it is also compositional dependent. For a given grain size, the J_{rs}/J_s ratio increases with increasing titanium content [*Day et al.*, 1977, *Cisowski*, 1980].

The behavior of NRM and IRM versus alternating field has also been checked [*Lowrie and Fuller*, 1971; *Dunlop*, 1983]. J_s was estimated from curves of the ratio J/H versus the applied field H, with a maximum field strength of 7.5 KG. In most cases, the paramagnetic contribution of other Fe-rich minerals, like olivine, produces a linear increase of the total moment at high fields. To account for this fact, we have extrapolated a straight line through the high field points on the J/H - H curves, back to zero field H.

Values of J_{rs} were determined by progressive IRM acquisition, up to maximum applied fields of 500-600 mT. In all cases, saturation was obtained for fields lower than 250-300 mT. The observed values of J_{rs}/J_s extend from 0.07 to 0.32, with an arithmetic mean value of 0.2 ± 0.06. A value of J_{rs}/J_s of 0.5 is predicted for uniaxial single-domain (SD) grains of magnetite; however, in basalt containing titanomagnetite, realistic SD or pseudo-single-domain (PSD) values are $0.17 \leq J_{rs}/J_s \leq 0.27$, while for multi-domain MD grains a ratio $J_{rs}/J_s <$ 0.1-0.13 is expected [*Dunlop*, 1981, 1983]. The distribution of J_{rs}/J_s ratios indicates that most of the selected samples contains SD or PSD grains and only a few have large magnetic particles.

Dunlop [1983] did study the behavior of a large collection of continental igneous rocks during A.F demagnetizations of remanences acquired in weak, intermediate, and strong fields (another kind of Lowrie-Fuller test). Remanences were either a TRM, anhysteretic remanent magnetization (ARM) or IRM. Four general categories of behavior have been recognized: MD-type: soft and rapidly decaying curves, with the IRM curves being hardest, which corresponds to MD grains above PSD threshold size. SD-type: harder, initially slowly decaying curves, the IRM curve being softest. This behavior is produced by SD and PSD grains. Transitional type: which produces closely spaced curves with or without crossovers. These curves correspond either to a single magnetic phase whose size spectrum peaks between SD (or PSD) and MD grains or to two phases with overlapping size spectra. Bimodal type: characterized by widely separated curves with SD-type relative hardness for weak field remanence, combining MD-type IRM curves. This behavior results of two phases, one MD, the other PSD or SD, with widely separated size spectra. The fine grains dominate weak field remanence, while the coarse grains dominate strong field remanence. [*Dunlop*, 1983].

Three of these four kinds of behavior were recognized in our 36 selected samples, for which the decay of the NRM (which is assumed to be the primary TRM) and the IRM have been compared. Examples of each sample type are given in Figure 7. It appears that SD-type samples have $J_{rs}/J_s > 0.23$, a median demagnetizing field (MDF) for the NRM: MDF_{NRM} >340 Oe and for IRM: $MDF_{IRM} > 225$ Oe. Their low-

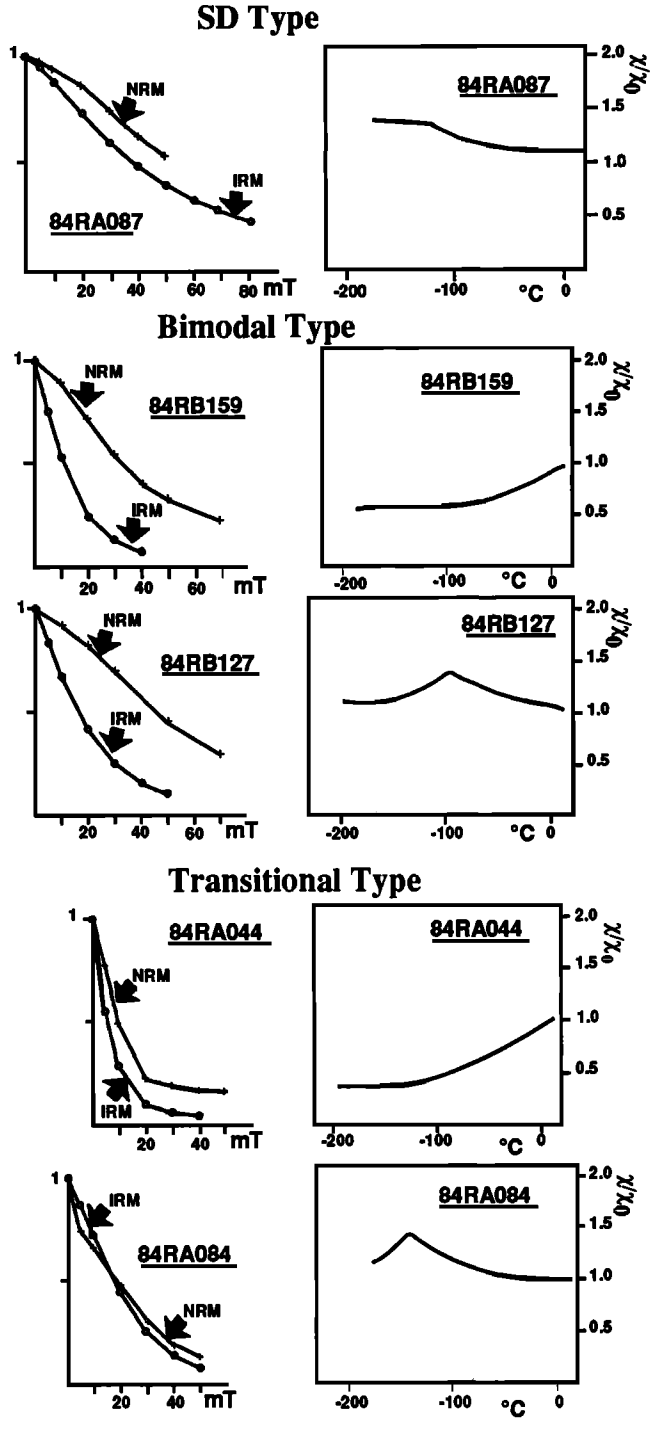

Fig. 7. Comparison of the AF demagnetization spectrum of NRM and IRM (left) with low temperature susceptibility (right). Three classifications, SD type, bimodal type, and transitional type are made according to the proposition of *Dunlop* [1983].

temperature susceptibility behavior follows group 2 of *Senanayake and McElhinny* [1981]. Curie temperatures for these samples are higher than 537°C (see Figure 4). Four samples belong to this category. Transitional-type samples show a J_{rs}/J_s ratio between 0.07 and 0.16 with two exceptions for which the value is higher and close to 0.21-0.25. Their MDF_{NRM} and MDF_{IRM} are between

60 and 220 Oe and their χ-T curves correspond to group 1 or 2 of *Senanayake and McElhinny* [1981]. Strong field thermomagnetic curves indicate either a single Curie point either higher than 530°C or lower than 120°C or two Curie temperatures (i.e., two magnetic phases) (see Figure 4). Fourteen samples are in this category. In the case of samples with low Curie points, it is easy to understand that these unoxidized titanomagnetites are larger magnetic particles. Bimodal type samples are the most common (18 samples). They exhibit J_{rs}/J_s ratio from 0.11 up to 0.31; 217< MDF_{NRM}< 500 Oe and 88< MDF_{IRM}<206 Oe. The low-temperature susceptibility behavior of these samples follows either group 1 or 3 of *Senanayake and McElhinny* [1981]. It appears, according to the thermomagnetic curves that these samples have either two Curie points (one lower than 200°, the other above 450°C) or only one Curie temperature (see Figure 4). We have not observed large MD-type behavior characterized by the IRM demagnetization curve above that of the NRM.

In conclusion, χ-T curves are compositional and grain size dependent; this result is in good agreement with those obtained in previous studies [*Senanayake and McElhinny*, 1981, 1982]. Thermomagnetic curves performed on almost even sample demonstrate the great variety in the composition and the oxidation state of our samples. Hysteresis properties have shown domain structure of either SD or PSD or a mixture of domain types.

However, all these experiments show the difficulty of selecting samples for paleointensity because there is a wide range with a continuous spectrum of magnetic properties rather then shape and clear class as suggested by Senanayake and McElhinny. We will see in the next section how magnetic properties could or could not explain some nonideal behavior during the Thellier experiment.

PALEOINTENSITY DETERMINATION

Experimental Procedure

The original method of paleointensity proposed by *Thellier and Thellier* [1959] is based upon the law of additivity of partial thermoremanent magnetizations (PTRM). At each temperature step, the specimens are heated twice at the same temperature T_i and cooled in the ambient geomagnetic field. Between these two heatings, the sample position is reversed 180° with respect to the direction of field. The total magnetization (residual NRM + PTRM) is measured after each heating. Because of the additivity of PTRMs, the two PTRMs acquired between T_i and room temperature are of the same magnitude but in opposite sense. This procedure enables one to recover the NRM left in the sample and the PTRM acquired. *Coe* [1967b] suggested performing the first heating in zero field in order to determine directly the NRM left. The second heating, performed in a field, enables one to measure the PTRM acquired. The Coe method has been widely used. *Kono and Ueno* [1977] have proposed a modified version of the Thellier's technique. It consists of only one heating at each temperature step with a laboratory field applied orthogonal to the NRM directions of the samples. However, even if this method is less time consuming, it requires a complex sample holder for a very precise orientation of the samples with respect to the applied field. Analysis of errors performed on both coordinates (NRM and TRM components) of the results of the Thellier experiments have shown that among the three previously mentioned versions, the original procedure is the most superior [*Kono and Tanaka*, 1984]. On the other hand, departures from additivity could have some effects in the Coe's version because the two heatings are not perfectly symmetrical [*Levi*, 1979]. For these reasons, we have chosen to use the original Thellier's technique and the laboratory field was reversed between the two heatings at each temperature step while the samples are left in the same position. This procedure allows a better repetition in the temperature reached by the sample if a low thermal gradient exists in the furnace. This repeatibility in temperature was about 1°. The laboratory field was applied both during heating and cooling as suggested by *Levi* [1975] and was adjusted to be close to the expected ancient field [*Tanaka and Kono*, 1984]. The samples were heated in a quartz tube evacuated to pressures less than 10^{-2} torr in order to prevent oxidation during heating [*Khodair and Coe*, 1975]. Each heating and cooling cycle lasted about 3 hours.

Generally, 11-20 temperature steps have been distributed in the range 100°C through the highest Curie point of the samples and distributed according to their unblocking temperature spectrum. One of the major advantage of Thellier's technique is that it allows a check of the stability of PTRM acquisition capacity as the temperature is progressively increased. Numerous PTRM checks were performed in two different ways: (1) by periodic measurements of the PTRM acquired at a given low-temperature interval, after previous heatings at higher temperature or (2) by successive PTRM checks spanning higher-temperature intervals as the temperature step increases [*Prévot et al.*, 1985].

Sample Selection

The most straightforward selection criterion is that the natural magnetization of the sample should have a direction close to the characteristic direction determined from several samples of the same flow. Samples with high Curie points and a good reversibility of the heating and cooling curves of the strong field experiment are generally assumed to be the most suitable samples for paleointensity determinations. It has also been suggested that large particles (MD grains) can produce nonideal behavior during Thellier experiments [*Levi*, 1977; *Worm et al.*, 1988]. Because MD grains are well known to have coercivities lower than 200 Oe [*Soffel*, 1971; *Levi and Merrill*, 1977], samples having MDF equal or above 300 Oe generally provide the most accurate paleointensity results.

No strict selection criterion has been used in order to perform experiments for most of the lava flows. On

the contrary, we will try to compare our extensive paleointensity experiments with the other available magnetic parameters in order to provide some additional constraints on sample selection for paleointensity.

Paleointensity experiments were attempted on 96 specimens and 66 provided results. Very few samples provided linear relation of NRM versus TRM over the whole temperature spectrum. Those which did not show any linear segment have been rejected.

Paleointensity Analysis

Choice of the points on the NRM-TRM diagram. Results of paleointensity experiments were reported in the classical NRM-TRM diagram. The interpretation of the NRM-TRM curves was conducted in the following way. Points must be distributed on a straight line in the temperature interval (T_{min}-T_{max}) chosen for paleointensity calculation. The minimum number of points used in calculating the paleointensity should be five with a corresponding fraction of NRM used being at least 15% of the initial NRM intensity [*Coe*, 1967b; *Prévot et a.*, 1985]. The minimum temperature (T_{min}) should be the one at which any secondary magnetization, such as a small VRM, is completely removed. The highest temperature (T_{max}) is defined as the temperature at which significant modifications of the magnetic mineralogy occur. Such magnetochemical changes can be detected by nonlinearity in the NRM-TRM curve, by changes in the PTRM checks, or by chemical remanent magnetization (CRM) acquisition. CRM buildup during heating is recognized if the applied field is not colinear with the existing NRM [*Coe et al.*, 1978, *Coe et al*, 1984]. Indeed, CRM is generally parallel to the applied field and has higher unblocking temperatures than the ones at which it was created. Thus the apparent residual NRM is the sum of the true residual NRM and the CRM vector. Another tool for recognizing magnetochemical changes is the measurement of the weak field susceptibility at room temperature after each heating.

Numerical analysis. The paleointensity was calculated using least squares fitting of a straight line [York, 1966, 1967] through the chosen NRM-TRM points. The reliability of a paleointensity determination was estimated from the NRM fraction (f) used in the calculation of the paleofield strength (Fe), the gap factor (g) and the scattering of the points about a linear segment [*Coe et al.*, 1978]. The quality factor (q) defined by *Coe et al.* [1978] is a function of these parameters ($q=bxfxg/\sigma_b$) with b being the slope of the straight line and σ_b the standard error of the slope. The weighted average paleointensities (<Fe>) within a single volcanic unit were computed using the weighting factor w defined by *Prévot et al.* [1985] ($w=q/\sqrt{(N-2)}$, where N is the number of points on the straight segment). An estimate of the potential for error caused by CRM acquisition is given for each sample by the factor R defined by *Coe et al.* [1984] $R=(CRM_{max}/\Delta TRM)x100$ (where ΔTRM is the portion of the TRM which defines the straight segment). It represents, in percent of the applied field, the maximum error that CRM would cause to the paleointensity determination.

Non Ideal Behavior During Thellier Experiments

In this section, we will describe briefly the various examples of nonideal behavior and compare the Thellier experiments with other available magnetic parameters. Some of them were determined on different specimens of a same core, and thus we make the assumption that the magnetic properties are homogeneous over the length of the core.

Effect of viscosity. Three samples which have a viscosity index above 5% (i.e., between 7 and 12%) did not provide any linear NRM-TRM curves. Also, these samples have Curie points below 400°C (type 4 J_S-T curves), and they exhibited low-temperature susceptibility behavior of type 1. These parameters as well as a low J_{rs}/J_S ratio determined on one sample suggest that they all have Ti-rich titanomagnetite with relatively large magnetic particles. These examples strengthen previous analysis [*Prévot et al.*, 1985], suggesting that viscous samples must be avoided from paleointensity experiments. Long-term viscosity acquired during the last thousand years may not be easily recognized because it is almost colinear with the primary normal TRM direction. Demagnetization of such a viscous led generally to concave up curvature of the NRM-TRM diagram [*Coe*, 1967b].

Susceptibility modifications. Generally, the weak field susceptibility increased during the first temperature steps up to 10% of its initial value. This increase seems to be a "stress" effect rather than reflecting mineralogical changes. Variations in the range ±20% are not easily correlated to remanence changes as already reported by *Coe* [1967b] and *Prévot* [1975]. Nevertheless, the largest susceptibility variations are generally associated to nonideal behavior during Thellier experiments. Also mineralogical changes appear to be more strongly related to temperature than to our experimental time durations. Changes of the weak field susceptibility always occur after the first heating at each temperature. The successive second heating at the same temperature step has very little effect and the susceptibility was almost always the same as after the first heating. On the contrary, an increase in temperature of a few tens of degrees at the next Thellier step is generally sufficient to make further susceptibility changes.

The systematic measurements of susceptibility during paleointensity indicate that no change in susceptibility is not always necessarily associated with good reliability of the paleointensity (Figure 8, sample RB160). But important changes in susceptibility always reflect a low thermal stability of the sample (Figure 8, sample RB141).

Increases in PTRM acquisition. The most common nonideal behavior is an increase in PTRM acquisition. Two examples are given in Figure 8. This behavior is probably due to the formation of titanomagnetite richer in iron and therefore more magnetic than the original one.

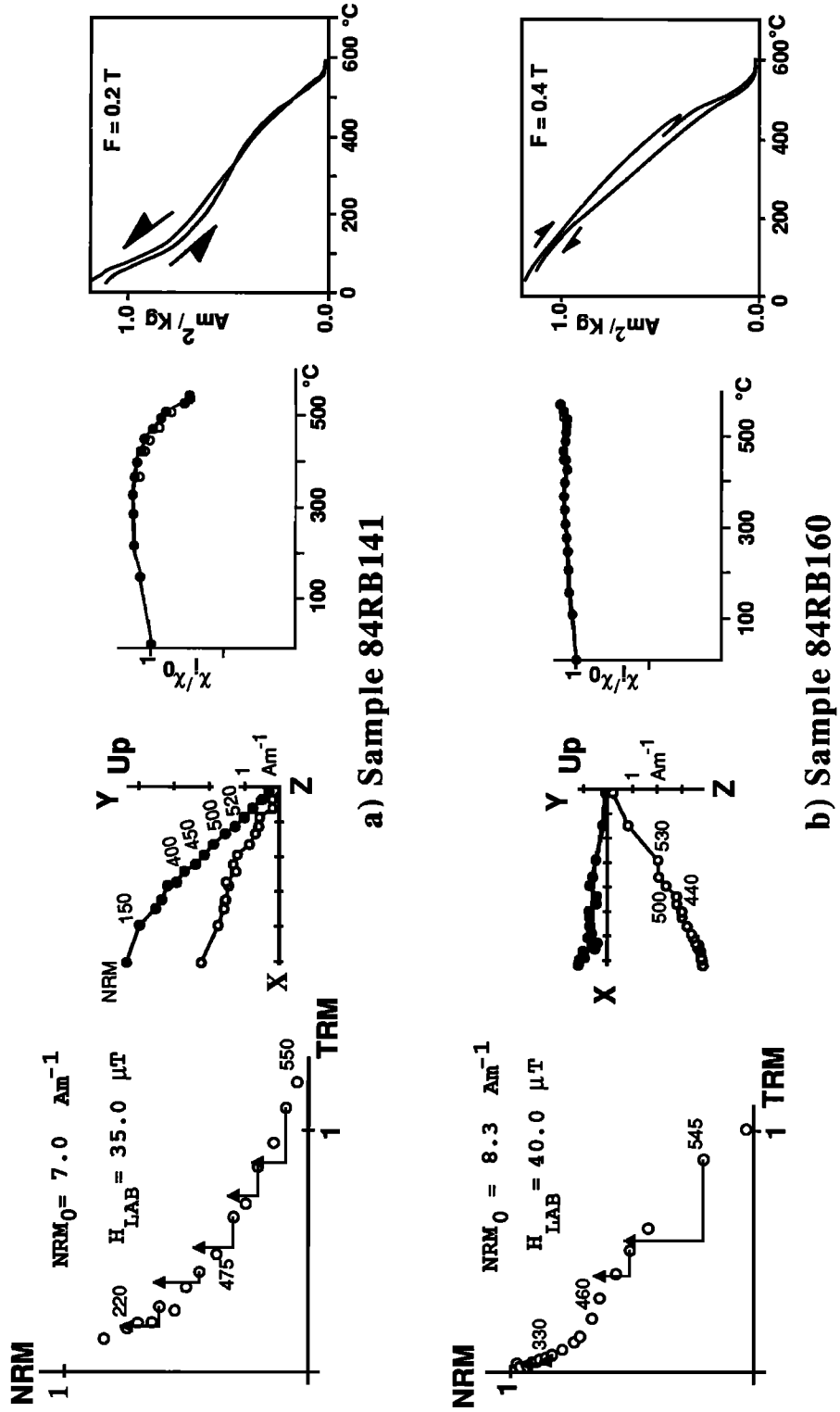

Fig. 8. Examples of increase in PTRM capacity during the Thellier experiments and comparison with the stability of the NRM direction, measurements of the room temperature susceptibility and J_s-T experiments. The NRM-TRM diagram is normalized with the initial NRM_0, and the triangles are the PTRM checks. H_{LAB} refers to the laboratory field. Temperature steps are in degrees Celsius. The solid symbols on the susceptibility diagrams correspond to the measurement after the first heating, while the open symbols indicate measurements after the second heating. These diagrams are normalized with the initial susceptibility (χ_0) measured before the first heating. Orthogonal plots of the NRM evolution are reported in sample coordinates.

CRM acquisition. Some samples have clearly shown deviations of the NRM direction toward that of the field applied during the first heating, a direction which was vertical down in sample coordinates (Figure 9). This is interpreted as the acquisition of a CRM parallel and in the sense of the field applied during the first heating at each temperature step. As it was already pointed out for samples which show significant susceptibility changes after heatings, the first heating is the most important. There is no clear correlation between CRM and the other magnetic data. The best examples (Figure 9) show no important variation of the susceptibility at room temperature and their J_S-T curves indicate a single high temperature Curie point (types 1a and 1b of Js-T curves, see Figure 4). However, information provided by low-temperature susceptibility and the Lowrie-Fuller test suggest large PSD grains.

Nonideal behavior characterized by a "kink". Kinks in the paleointensity diagram have been observed for 11 samples. They are defined as a large drop in the NRM intensity without any acquisition of laboratory TRM, in an intermediate temperature interval, 200°-400°C (Figure 10). This kind of behavior was already reported by *Bogue and Coe* [1984]. PTRM checks indicated first a decrease followed at higher temperatures by an increase in PTRM capacity. Such a 'kink' was found on samples with one or two Curie points. The reversibility of the heating and cooling thermomagnetic curves was variable. These samples have χ-T curves following group 1 or 3 of *Senanayake and McElhinny* [1981], and the shape of the demagnetization of the NRM and IRM suggest that they are bimodal or transitional-type samples. The largest changes of room temperature susceptibility, measured after each heating, are observed within this group of samples (Figure 10).

Non ideal behavior and J_S-T curves. Samples which have two magnetic phases have often shown poor reliability in paleointensity experiments. Sample RB141 (Figure 8) is one of these. It is not easy to correlate quantitatively J_S-T curves with paleointensity quality. Instead, we have compared the temperature at which half of the natural remanence is demagnetized (MDT) with the quality factor q of the paleointensity experiment. Three classes have been identified (Figure 11). It is clear from Figure 11 that samples which have the best behavior in paleointensity (q>10) have high and narrow unblocking temperatures while low-quality samples and rejected samples have MDTs which indicate intermediate unblocking temperatures. However, a few samples from flows with only one well-

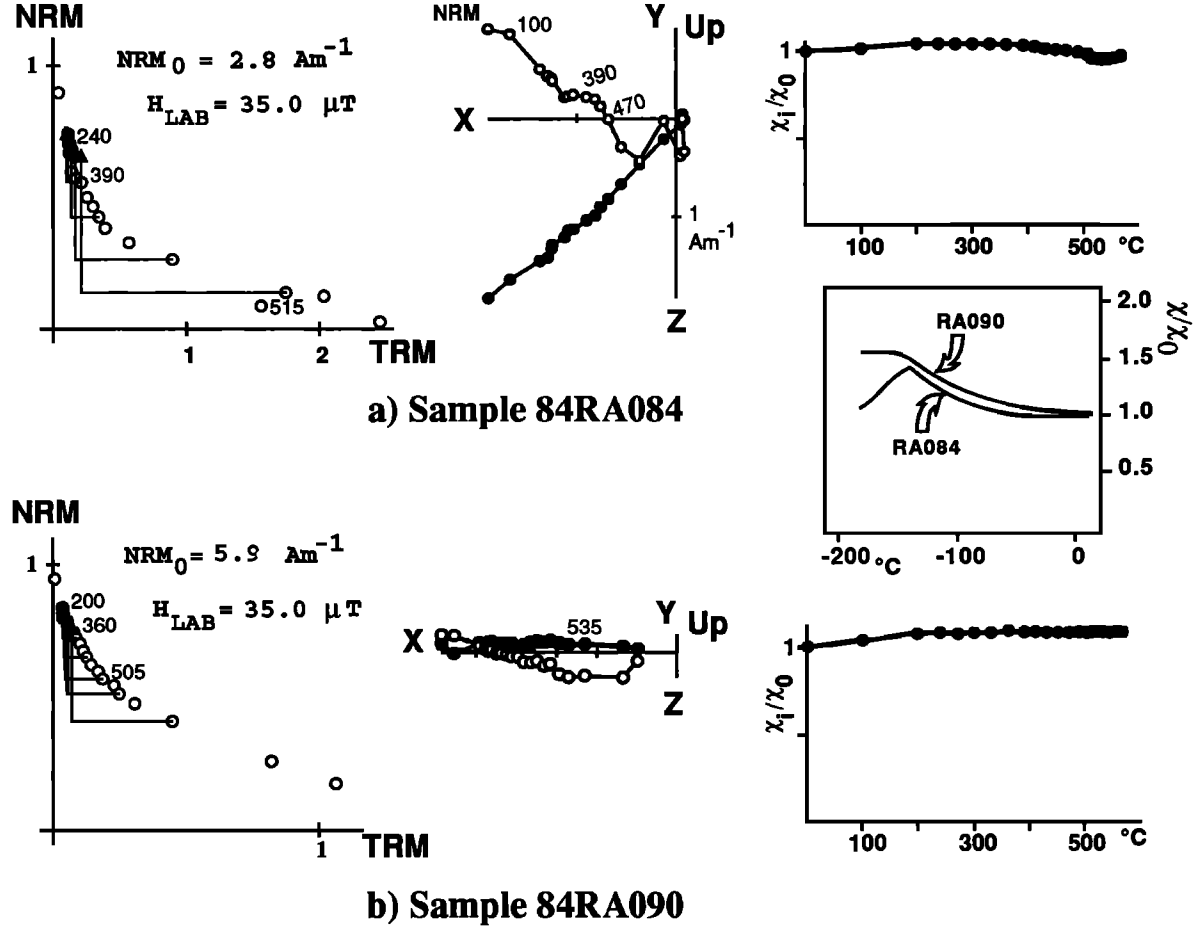

Fig. 9. Same conventions than in Figure 8. The NRM direction does not decay through the origin but rather is deviated toward the direction of the applied field which was vertical down in sample coordinates. The variation of the susceptibility at low temperature is also given.

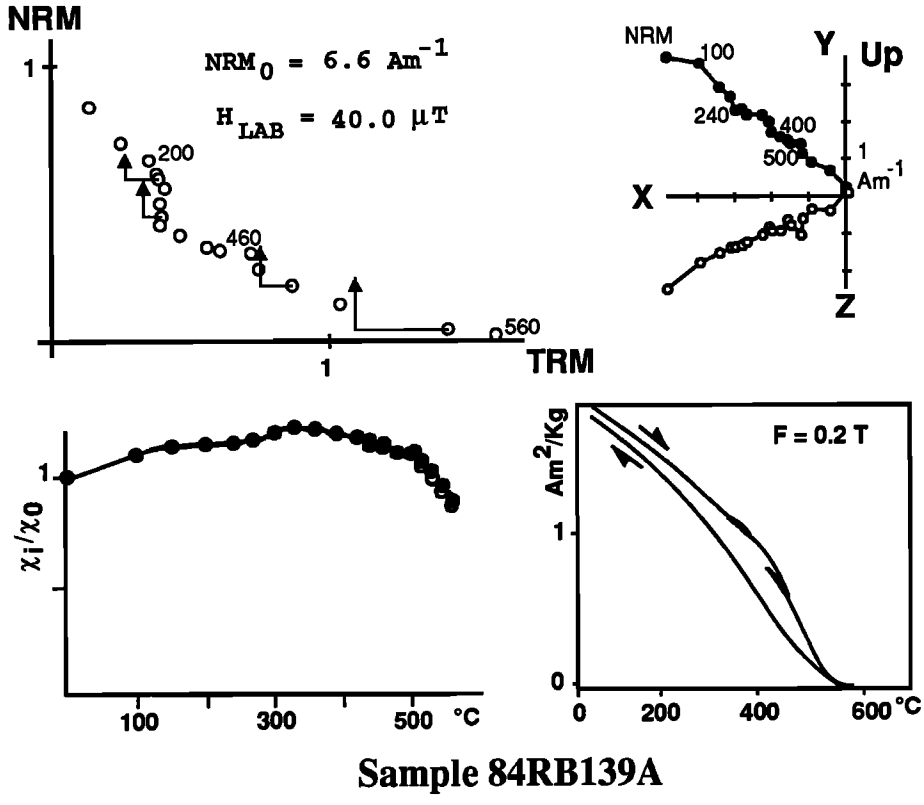

Fig. 10. The NRM-TRM diagram is characterized by a "kink" with a large decrease in NRM without any TRM acquisition in the temperature range 200°-400°C.

defined low Curie point have also provided successful paleointensity results.

Magnetic changes observed during J_S-T experiments do not always occur in the same way during paleointensity experiments. An example is given by sample RB138 (Figure 12) for which J_S-T experiments were performed before and after a paleointensity experiment. While during the initial J_S-T experiment, mineralogical changes did correspond to a small reduction, with a decrease of a few degrees in both low and high Curie points, on the contrary, after paleointensity the Js-T experiment shows that the numerous paleointensity heatings resulted in a slight oxidation of the sample. Some opposite behaviors have also been found. Thus it is not easy to interpret nonideal behavior during paleointensity in light of the kind of reversibility of J_S-T curves, possibly because the experimental heating conditions are not identical in both experiments.

We can conclude that the best candidates for paleointensity are the high temperature oxidized samples with high unblocking temperatures, but we will see later that samples with a single well-defined low-temperature Curie phase should not be systematically rejected.

Concave up behavior. In some cases, the NRM versus TRM points are distributed on a curve for which two line segments can be defined (sample RB134, Figure 13) and for which there is no indication of mineralogical alterations. It has been suggested that multidomain grains contribute to this curvature [*Levi*, 1977]. The χ-T curves provide some indication of grain size. An example is given by four experiments conducted on flow RB4. Samples RB128 and RB129 which do not show the magnetite peak transition have provided very convincing paleointensity results (see Table 2), while samples RB131 and RB134 show some evidence of larger grain size and they provided concave-up curvature. Selecting the lower-temperature interval is one basis of the Thellier method, in this situation, because it is well known that alteration increases with increasing temperature. However, because of multidomain grain effects, it is sometimes also tempting to fit the line through an intermediate temperature interval. This will provide a paleointensity value approximately quarter of that using the low temperature spectrum (Figure 13). The curvature was less pronounced for sample RB131 which we did not reject. As a result, it provides a slightly higher paleointensity value. However because of its lower quality value, it did not have much weight in the flow average. The grain size difference suggested by the low-temperature susceptibility curves was not observed with AF demagnetization which provided MDF greater than 30 mT.

In the analysis of the Réunion data, in the case of ambiguous samples, we choose the first approach (i.e., fitting the line through the lowest temperature interval

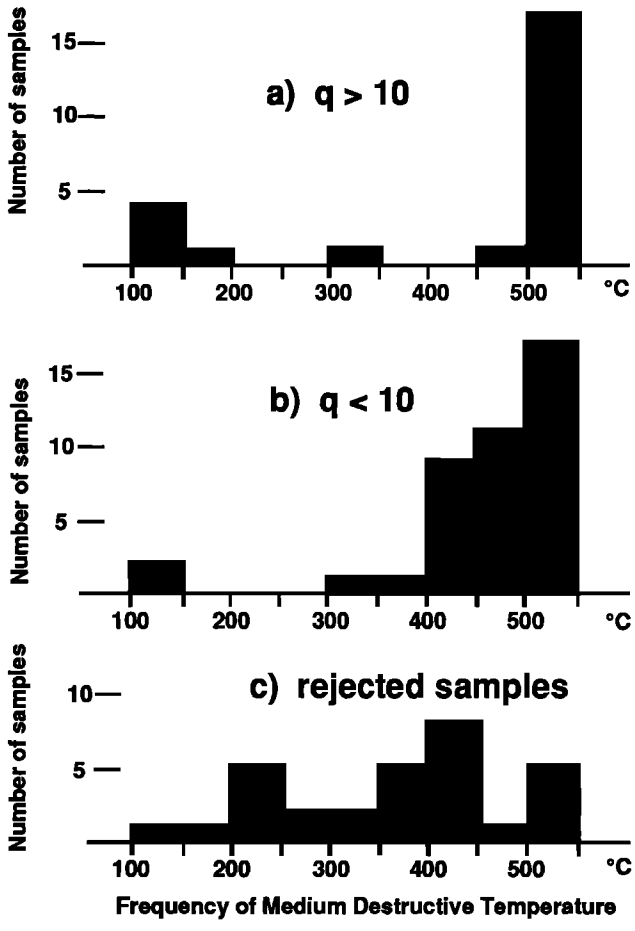

Fig. 11. Distribution of the MDT (medium destructive temperature) for two classes of samples according to the value of the quality factor (q) of the paleointensity experiments and for samples for which the paleointensity diagrams were rejected.

like with sample RB131, Figure 13) which seems to be the more rigorous. However, for such samples, the curve is fitted using a small NRM fraction, and thus the quality factor is also low. As a consequence, discussions about paleointensity variations should be keep in mind the importance of the quality factor. Also, we shall emphasize that paleointensity experiments should be performed up to an almost complete demagnetization of the NRM, allowing a better assessment of the true complete behavior of the sample.

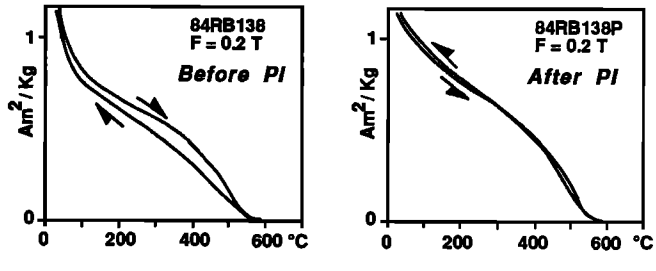

Fig. 12. Comparison of thermomagnetic experiments performed in vacuum before and after a paleointensity experiment. The low Curie point shown by the first experiment is much less clear after the paleointensity.

In brief, it seems that concave-up NRM-TRM plots and diagrams characterized by a kink are preferentially observed on samples showing some evidence of larger grain size (large PSD or MD grains). If CRM acquisition and increases in PTRM acquisition appear difficult to correlate with a specific magnetic property, it is clear that samples with a viscosity index above 5% must be rejected.

Paleointensity Results (Table 2)

Reliability of the results. The standard error of a single paleointensity determination as well as the standard deviation of a mean paleointensity per flow do not take into account several sources of uncertainties. They represent only the analytical precision of the result. Such uncertainties were already discussed by *Coe* [1967a,b], i.e., development of magnetochemical changes which have not been recognized, the human bias in selection of the temperature interval, especially in the case of concave-up behavior and the effect of cooling rate on the TRM intensity.

Theoretical studies have predicted that for an assemblage of SD grains of magnetite, an increase of 5-10% of the TRM intensity when cooling rate decreases by one order of magnitude [*Dodson and McClelland-Brown*, 1980; *Halgedahl et al.*, 1980]. Such effects were recognized on synthetic [*McClelland-Brown*, 1984] and natural samples [*Fox and Aitken*, 1980]. Experiments were conducted to check the effect of cooling rate for six basalt samples from La Réunion. These samples have magnetite Curie points, high unblocking temperatures, and MDF values above 30 mT. All heatings were performed in vacuum in a laboratory field of 50 μT. Samples were first given a full TRM by cooling from 650°C to room temperature over 1 1/4 hour. During this cooling, temperature decreases from 650°-400°C in almost 4 min (that is about 40°C/min). The magnetic moment M0 measured at room temperature was taken as reference. Then two experiments (S1 and S2) with lower cooling rate were performed.

A decrease in temperature of 8°C/min between 650° and 400°C was used during the first experiment (S1) with a complete cooling to room temperature taking about 8 hours.

The second (S2) corresponds to a slower cooling of 1°C/min between 650° and 400°C.

Two remagnetizations (M1 and M2) with an identical procedure as the initial one (M0) were carried out after each of the slow cooling experiments in order to check that no important chemical alteration occurred during heatings. Results shown in Figure 14 indicate the good thermal stability of the samples with TRM intensity variations (M1-M0; M2-M0) about ±2% of the initial TRM (M0). In contrast, the effect of cooling rate is clearly significant and characterized by the increases in TRM acquisition. The maximum increase is observed after the experiment with the lowest cooling rate. However, the amount of increase varies from 5 to 14%, and this suggests cooling rate dependency upon mineralogical properties. For example, samples with the

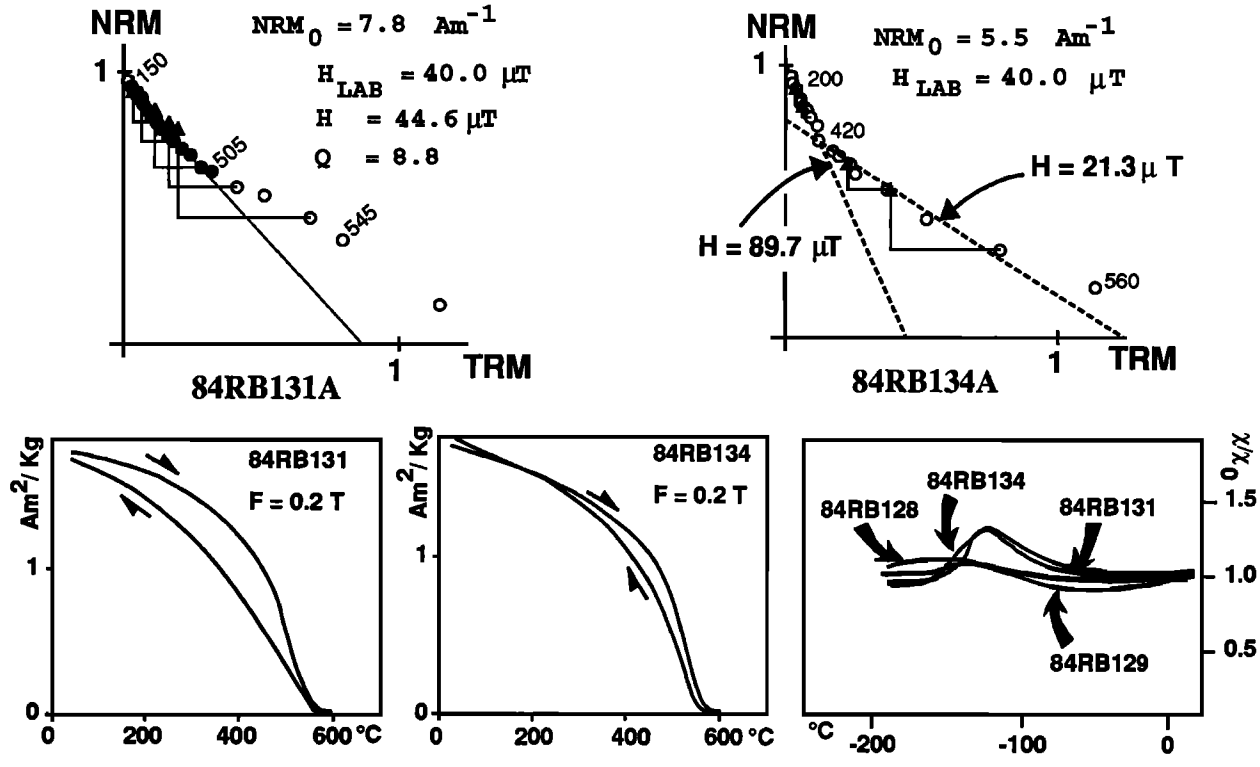

Fig. 13. Examples of concave-up behavior for two samples of a same flow (RB4). The dashed lines (sample RB134) correspond to two different interpretations of the NRM-TRM diagram. For sample RB131, the solid circles correspond to the points used for the paleointensity calculation. J_S-T curves indicate a single magnetic phase close to pure magnetite. Samples RB131 and RB134 exhibit at low temperature the peak of the magnetite magnetocrystalline transition which is not observed on two other samples from the same flow (samples RB128 and RB129). H_{LAB} is the laboratory field.

highest blocking temperatures (samples 1 and 2, Figure 14) are the least sensitive to the effect of cooling rate.

Strong anisotropy of samples, as it is sometimes observed on archeomagnetic material, should lead to important errors in the paleointensity determination [*Aitken et al.*, 1981]. For lava flows, the expected anisotropy is low. In order to check this point, the average inclination of TRM measured during the last two heatings of the Thellier experiment was calculated for the 66 samples which have given reliable results. As the laboratory field was applied along the Z axis of samples, an inclination close to 90° is expected. In 87% of cases, the TRM inclination was greater than 87.5°. This small deviation should be the result of a very low anisotropy and a small inaccuracy in the positioning of samples within the oven. On five samples, deviations of TRM between 4° and 6° were observed.

Because of all sources of uncertainty during the Thellier's experiment indicated above, we must emphasize that even if analytical errors are low (i.e., less than 5%), the true error is probably ±10-30% of the true paleofield strength, according to samples.

Typically, the NRM fraction f reported in Table 2 varies from 0.15 to 0.9 and the quality factor q ranges from 1.2 to 91.2. The average number of points N which defines the straight line of the paleointensity data is close to 10. A strong correlation is observed between f and q (Figure 15). Thus care must be taken by researchers not to increase artificially the factor q by increasing f in keeping points which may be off the line.

Differences in grain size between samples can be estimated from the laboratory Koenisberger ratio Q_L, defined by *Prévot et al.* [1985]; Q_L=k(TRM)/χ, where χ is the magnetic susceptibility before heating and k(TRM) is the total TRM intensity that would be acquired, in the absence of any magnetochemical changes, in a field equal to unity. Data from the Steens Mountain have shown a clear correlation between Q_L and the maximum temperature (T_{max}) usable for paleointensity determination, before the beginning of magnetochemical changes. For values of T_{max} between 400 and 600°C, no such clear correlation is observed in our results between Q_L and T_{max}. However, the lowest values correspond to T_{max} below 500°C (Figure16).

Description of the results. The variation between samples for a single unit is often larger than each individual error estimate thus demonstrating the need of several determinations per flow. We present successively the data for site B and then site A.

Forty-six samples from the site B (Remparts de Bellecombe) were studied. Paleointensity results have been obtained for 10 flows among 13, with at least two determinations per flow. The exception is flow RB8 for which three experiments were attempted and only one was successful. High-quality linear NRM-TRM diagrams

TABLE 2 Paleointensity Results

Lava Flow	Sample	D	I	Tc °C	Js-T Type	J_{NRM} A m^{-1}	H_L	N	∂T	f	g	q	r	$\%R$	Q_L	Fe±σFe μT	Fe±s.d. μT	<Fe> μT	VDM A m^2
									Site B Remparts de Bellecombe										
RB1	RB108	6.0	-37.0	505	3c	5.2	35	7	200-440	0.274	0.797	1.6	0.950	13.7	35.4	36.6±5.5			
	RB109	5.0	-40.0	514	1b	16.3	40	9	330-480	0.174	0.866	2.8	0.990	2.1	39.3	37.5±1.7			
	RB110	1.2	-35.8	526	1b	9.3	35	5	250-410	0.178	0.738	1.9	0.993	20.5	17.0	37.2±2.5	37.1±0.5	37.2	7.9
RB2	RB113	12.0	-35.8	523	1e	8.8	40	13	200-480	0.295	0.901	3.3	0.964	15.8	13.7	54.7±8.3			
	RB114	0.3	-35.7	516	1a	8.5	35	11	200-530	0.575	0.858	11.4	0.992	12.6	16.5	50.8±2.2			
	RB115	nd	nd	531	1a	8.0	35	13	300-540	0.503	0.880	14.4	0.995	18.6	15.3	55.2±1.7			
	RB116	2.0	-34.0	465	1c	5.8	35	6	200-410	0.234	0.783	1.8	0.979	11.9	7.2	48.7±5.0			
	RB117	354.0	-34.0	547	1b	13.4	35	8	370-520	0.610	0.818	20.5	0.998	9.2	13.4	38.7±0.9	49.6+6.7	46.4	9.8
RB3	RB119	0.9	-37.5	506	1b	7.7	40	15	240-560	0.819	0.846	31.2	0.997	5.0	16.2	26.9±0.6			
	RB120	0.5	-29.0	531	1a	16.6	35	15	200-540	0.552	0.841	24.5	0.998	11.4	25.9	37.6±0.7			
	RB121	355.0	-31.0	536	1d	11.0	40	14	270-560	0.870	0.857	53.6	0.999	4.0	37.3	36.7±0.5	33.7±5.9	34.2	7.8
RB3'	RB124	4.0	-36.0	540	1c	6.5	40	14	240-545	0.708	0.861	32.4	0.998	4.7	15.2	34.0±0.6			
	RB125	0.0	-34.5	542	1c	10.7	35	9	370-530	0.439	0.826	16.3	0.998	6.5	44.4	37.4±0.8			
	RB127	357.6	-38.3	530	1c	12.8	40	14	240-545	0.814	0.841	33.2	0.997	4.1	20.2	33.2±0.7	34.9±2.2	34.5	7.5
RB4	RB128	5.0	-35.3	514	1a	10.6	35	13	290-550	0.844	0.894	61.0	0.999	2.9	22.7	32.4±0.4			
	RB129	2.4	-30.0	510	1b	9.3	35	11	330-540	0.868	0.871	91.2	0.999	2.6	17.7	33.9±0.3			
	RB131	354.0	-28.5	519	1b	7.8	40	16	150-505	0.331	0.921	8.8	0.992	9.9	9.9	44.6±1.5	37.0±6.7	33.9	7.6
RB8	RB154	6.0	-50.0	533	1d	10.3	40	20	200-555	0.802	0.924	74.3	0.999	4.3	15.6	42.6±0.4	42.6±0.4		
RB9	RB158	2.0	-35.5	545	3a	8.4	40	10	240-480	0.420	0.875	7.3	0.990	4.9	25.8	34.6±1.7			
	RB159	10.0	-40.0	511	3a	6.4	40	11	150-435	0.416	0.888	6.1	0.983	9.4	12.2	48.1±2.9			
	RB161	355.0	-43.5	509	3a	8.8	35	13	290-550	0.910	0.882	52.1	0.999	3.0	29.9	36.5±0.6	39.7±7.3	37.4	7.8
RB10	RB164	340.0	-50.0	507	1b	11.1	40	11	240-500	0.374	0.858	5.4	0.984	8.3	11.3	47.1±2.8			
	RB165	355.0	-50.0	513	1a	9.8	40	11	240-500	0.348	0.868	5.3	0.985	9.6	11.3	45.7±2.6			
	RB166	9.0	-46.5	510	1c	11.5	40	14	150-480	0.252	0.894	6.3	0.992	3.8	13.7	40.6±1.4	44.5±3.4	44.4	8.6
RB11	RB169	351.0	-55.0	501	1c	8.2	35	7	100-410	0.344	0.710	3.0	0.984	7.9	6.0	48.4±3.9			
	RB170	355.0	-57.0	546	3a	6.2	40	9	240-435	0.283	0.831	2.9	0.978	9.7	23.1	33.1±2.6			
	RB161	354.0	-45.0	541	3a	10.4	35	7	200-440	0.233	0.813	2.1	0.980	7.3	18.1	40.3±3.6	40.6±7.7	41.2	7.6
RB12	RB173	330.0	-52.5	463	1a	7.7	35	6	250-440	0.220	0.699	1.3	0.972	19.3	4.9	55.4±6.5			
	RB175	353.0	-53.0	477	1a	11.2	35	7	290-475	0.266	0.769	2.3	0.980	15.7	11.1	35.1±3.1			
	RB176	350.0	-50.0	497	1a	10.6	40	10	240-450	0.170	0.852	2.4	0.986	10.5	10.8	47.2±2.8			
	RB177	353.0	-54.0	497	1a	9.5	35	6	250-440	0.155	0.703	1.2	0.986	16.7	10.5	37.8±3.2	43.1±9.3	43.1	7.9

TABLE 2 Paleointensity Results (continued)

Lava Flow	Sample	D	I	Tc °C	Js-T Type	J_{NRM} A m^{-1}	H_L	N	∂T	f	g	q	r	%R	Q_L	Fe±σFe μT	Fe±s.d. μT	<Fe> μT	VDM A m^2
Site A Rivière des Remparts																			
RA1	RA002	1.3	-47.8	538	1a	16.4	35	17	300-575	0.873	0.892	20.4	0.900	1.6	21.7	34.7±1.3			
	RA005	358.0	-44.5	519	1c	7.7	35	10	300-510	0.425	0.858	5.7	0.983	17.6	6.8	41.0±2.6	37.9±4.5	36.4	7.4
RA2	RA009	8.5	-47.0	552	1c	13.8	35	18	270-575	0.816	0.881	21.8	0.991	4.6	26.3	32.8±1.1	32.8±1.1		
RA3	RA011	4.5	-38.5	499	1e	10.7	35	14	200-515	0.593	0.905	16.8	0.994	5.9	12.0	33.1±1			
	RA013	19.0	-41.0	513	1a	13.1	35	11	200-490	0.445	0.856	7.6	0.989	5.8	14.7	26.2±1.3			
	RA014	nd	nd	491	1b	12.0	35	9	220-500	0.250	0.851	4.5	0.992	11.1	20.9	27.7±1.3			
	RA015	nd	nd	506	1b	8.2	35	11	340-530	0.460	0.861	6.7	0.984	5.3	17.5	33.5±2.0			
	RA017	nd	nd	527	1b	5.6	35	6	220-425	0.198	0.782	2.4	0.992	13.2	20.1	42.2±2.7	32.5±6.3	31.9	6.6
RA4	RA020	20.0	-55.0	117	2	3.2	35	6	70-135	0.618	0.750	14.5	0.998	6.1	5.9	58.6±1.9			
	RA021	6.2	-63.0	115	2	2.9	35	5	55-115	0.559	0.641	8.0	0.997	6.0	5.9	49.3±2.2	54.0±6.6	55.0	8.8
RA5	RA024	1.0	-56.0	131	2	4.6	35	12	70-215	0.679	0.895	16.6	0.993	14.1	8.9	53.9±2.0			
	RA026	358.5	-55.0	537	1c	3.9	35	7	150-425	0.459	0.825	6.9	0.992	9.1	5.2	59.2±3.3			
	RA027	357.0	-57.5	538	3a	4.9	35	14	70-240	0.244	0.897	3.5	0.976	19.1	12.5	40.7±2.5	51.3±9.5	54.2	8.8
RA6	RA030	355.0	-56.0	146	2	5.4	35	12	70-215	0.761	0.865	16.4	0.992	8.8	12.2	43.1±1.7			
	RA031	1.0	-53.5	n.d.	n.d.	3.8	35	10	70-175	0.596	0.833	11.3	0.992	8.3	6.9	47.4±2.1			
	RA032	352.0	-53.5	142	2	3.7	35	14	70-290	0.675	0.879	15.0	0.991	8.4	9.6	44.9±1.8			
	RA033	358.0	-55.0	138	2	3.1	35	5	70-145	0.624	0.795	6.5	0.985	10.8	4.2	58.4±4.4	48.5±6.9	47.9	8.1
RA7	RA038	16.0	-49.0	550	1c	2.2	35	7	200-410	0.433	0.811	4.7	0.986	14.6	2.4	47.3±3.5			
	RA039	355.0	-56.0	543	1c	3.7	35	9	200-430	0.454	0.844	7.0	0.989	7.3	5.4	41.8±2.3			
	RA040	8.9	-55.0	536	1a	4.4	35	8	220-475	0.561	0.850	5.6	0.978	12.8	4.9	47.4±4.1	45.5±3.2	45.3	8.0
RA9	RA047	350.0	-50.0	534	1a	2.6	35	9	240-450	0.316	0.845	2.7	0.965	14.3	1.8	48.3±4.8			
	RA048	348.0	-54.0	536	1a	2.6	35	9	200-450	0.376	0.861	4.2	0.979	20.5	2.0	48.1±3.7			
	RA049	10.0	-59.0	527	1b	2.9	35	8	220-475	0.520	0.820	3.9	0.965	17.0	2.9	37.5±4.0			
	RA051	358.0	-50.0	531	1b	2.8	35	9	200-450	0.343	0.840	2.7	0.961	22.5	2.7	43.3±4.6	44.3±5.1	44.0	7.7
RA10	RA053	2.0	-46.0	555	1a	14.3	35	8	400-530	0.314	0.805	6.9	0.996	11.3	28.7	33.1±1.2			
	RA057	8.0	-49.0	546	1a	14.2	35	7	370-510	0.241	0.811	2.7	0.987	16.8	20.4	43.2±3.1	38.2±7.1	36.1	7.2
RA11	RA064	4.6	-54.0	557	1c	12.1	35	17	200-570	0.946	0.793	39.8	0.997	7.2	26.8	30.0±0.6			
	RA066	6.0	-47.5	499	1a	5.1	35	20	200-575	0.873	0.924	47.1	0.997	2.1	12.3	28.8±0.5	29.4±0.8	29.4	5.5
RA13	RA073	340.0	-39.0	534	1d	2.5	35	7	300-450	0.293	0.825	2.5	0.977	14.6	4.9	29.6±2.8			
	RA077	327.0	-38.0	536	1a	3.3	35	7	240-410	0.445	0.825	5.7	0.990	14.1	3.2	31.1±1.6	30.4±1.1	30.6	6.3
RA15	RA086	336.5	-38.0	551	1d	3.5	35	15	200-525	0.406	0.881	9.2	0.990	14.9	8.0	26.0±1.0			
	RA087	344.0	-38.0	564	1d	1.1	35	14	200-530	0.559	0.895	26.9	0.998	9.6	25.7	16.7±0.3	21.4±6.6	19.0	4.1
RA17	RA099	16.5	-22.0	484	1e	5.3	35	8	220-475	0.231	0.837	2.6	0.983	13.7	3.1	43.8±3.3			
	RA100	353.0	-37.0	517	1b	3.8	35	9	200-450	0.368	0.863	4.4	0.982	14.0	2.0	37.0±2.6			
	RA105	5.0	-37.0	551	3a	5.0	35	17	85-485	0.832	0.872	15.3	0.983	8.8	5.5	53.4±2.5	44.7±8.2	47.8	9.9

D, I, mean magnetic declination and inclination of the NRM left in the ∂T interval; for some broken cores, the direction is not available; T_C, Curie temperature of the sample; J_S-T, type of the thermomagnetic curve; J_{NRM}, intensity of the natural remanence in A m^{-1}; H_L, intensity of the laboratory field in μT; N, number of points in the ∂T interval; ∂T, interval of temperature used the determine the paleointensity; f, g, q, NRM fraction, gap factor, and quality factor respectively [*Coe et al.*, 1978]; r, linear correlation coefficient; %R, maximum percentage of CRM [*Coe et al.*, 1984]; Q_L: laboratory Koenigsberger ratio; Fe, σ(Fe), paleointensity estimate for individual specimen in μT, and its standard error, Fe±s.d., unweighted average paleointensity of individual lava flow in μT, plus or minus its standard deviation; <Fe>, weighted mean in μT; VDM, virtual dipole moment in 10^{22} A m^2; n.d., not determined.

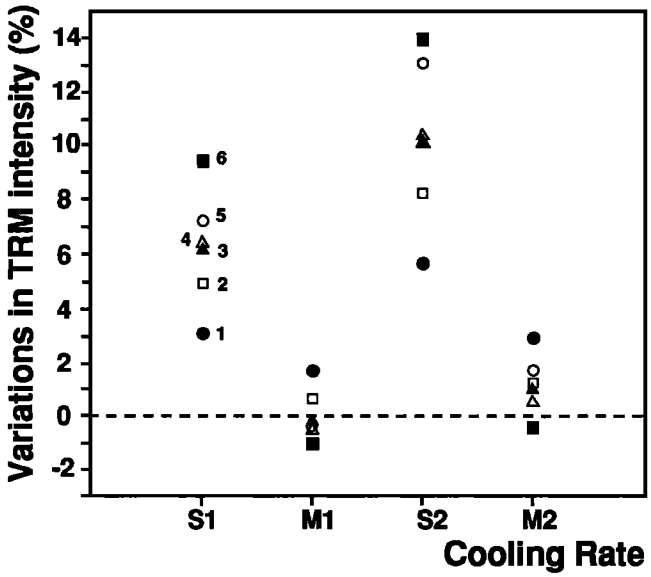

Fig. 14. Effect of cooling rate on the TRM intensity for six samples of basalts from La Réunion. M1 and M2 experiments correspond to fast cooling rates while S1 and S2 are slow cooling rates (see text).

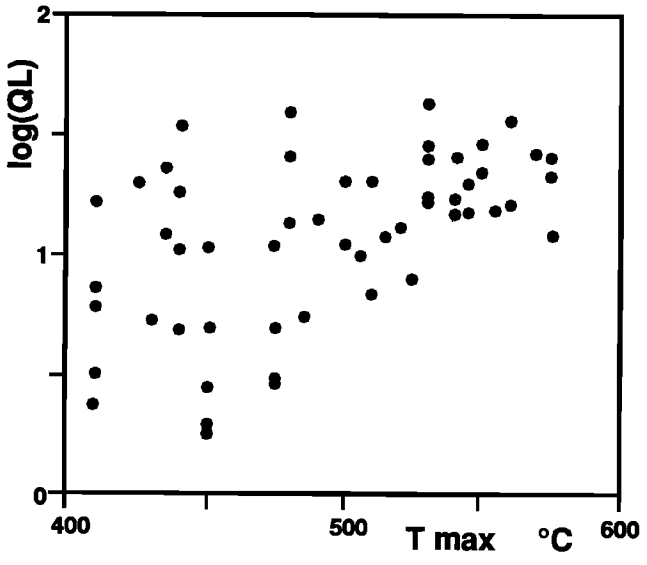

Fig. 16. Plot of the logarithm of the laboratory Koenigsberger (Q_L) versus the maximum temperature of the interval for paleointensity calculation (T_{max}).

have been obtained on some flows, and 13 samples have a quality factor greater than 10. An example is given with sample RB129 (Figure 17). Some other samples provided results with intermediate quality, like samples RB164 (Figure 17). Paleointensities with low-quality factors ($q \leq 3$) have been obtained for three flows RB1, RB11 and RB12, and these paleointensities are certainly less reliable. The scatter of the points on the straight line which defines the paleointensity slope is commonly low (see the coefficient of linear correlation r in Table 2).The paleointensities range from 34 to 46 μT.

Fifty samples from the site A (Rivière des Remparts) were studied, and 35 have given reliable results. Average paleointensities were obtained on 12 flow, among the 17 which compose the site. Only one result was acquired on flow RA2. It was not easy to find suitable samples for paleointensity determinations at this site, because of the existence of larger secondary components of magnetization. Some examples of paleointensity diagrams are given in Figure 18.

Samples composed of nonoxidized titanomagnetites

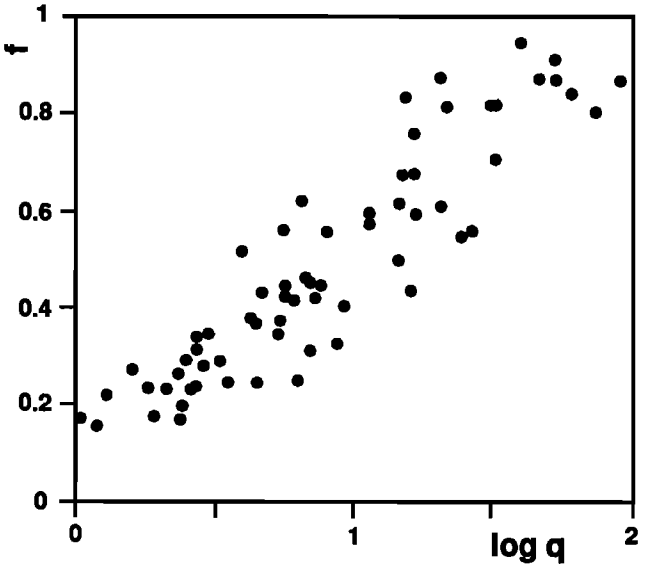

Fig. 15. Plot of the NRM fraction (f) used in the paleointensity determination versus the logarithm of the quality factor (q). A strong correlation is observed.

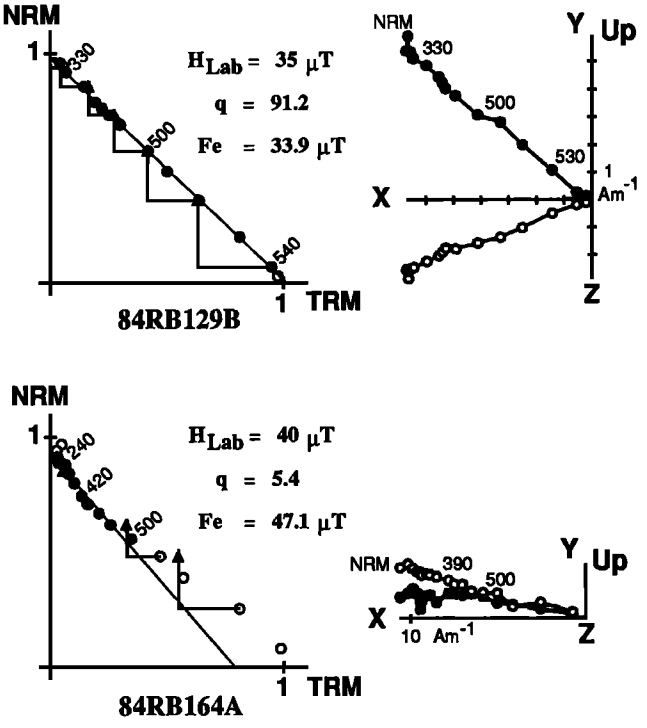

Fig. 17. Examples of successful paleointensity experiments for two samples from site B. H_{LAB} is the laboratory field, q is the quality factor, and Fe is the paleointensity estimate. The NRM demagnetization is shown in sample coordinates.

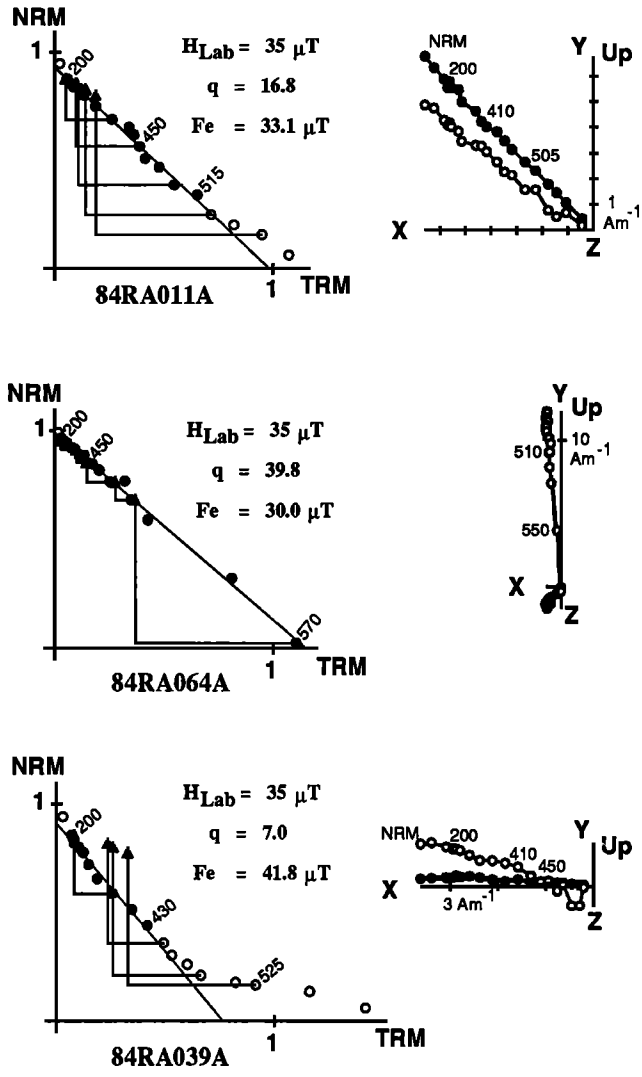

Fig. 18. Examples of reliable paleointensities for three samples from site A.

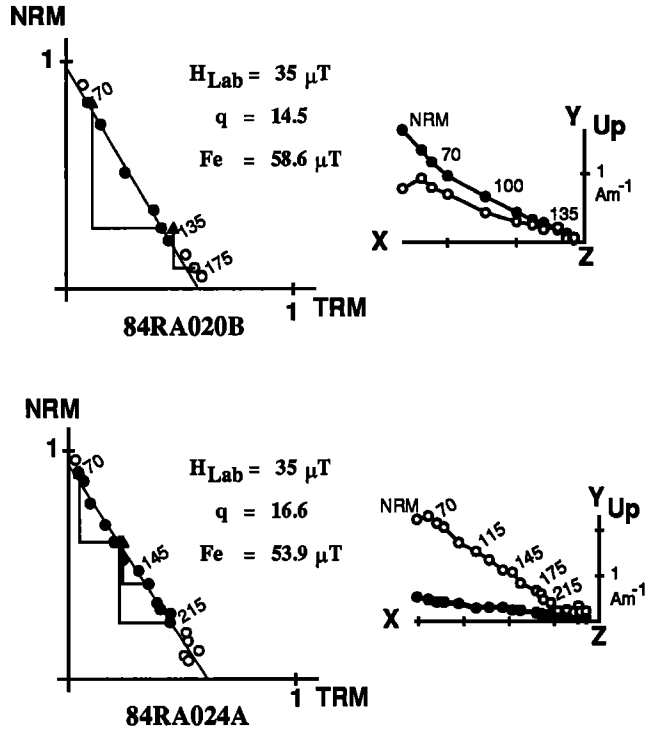

Fig. 19. Examples of reliable paleointensities for two samples with low unblocking temperatures due to Ti-rich titanomagnetites.

(type 2 J_S-T curves), were found on lava flows RA4, RA5, and RA6. As they did not carry important VRM or other overprints, Thellier experiments were performed on seven samples (Figure 19 and Table 2). Usually more than 50% of the initial NRM intensity was used for the paleointensity determination, before any magnetochemical change was observed. However, it has been shown that linearity of NRM against TRM as well as no change in PTRM capacity are not sufficient to prove the absence of physical or chemical changes in the temperature range used to calculate the strength of the paleofield [*Prévot et al.*, 1983]. In order to check that no important alteration of the sample magnetic mineralogy did occur during Thellier experiments, we have compared, the J_S-T curves performed before and after paleointensity measurements. Differences in Curie point are not important (Figure 20). No change is observed for sample RA021, while an increase of 14°C and a decrease of 13°C were observed for samples RA020 and RA033, respectively. During Thellier experiments, samples were heated at temperatures higher than the maximum temperature used to define the linear segment; the observed difference in Curie points may be the result of an alteration which may have started only at the end of the paleointensity experiments, as shown by PTRM checks (Figure 19). Therefore, we think that the temperature intervals used for the calculation are free of any magnetochemical changes. This check was important, because the highest paleointensity values for the site A were obtained on samples with low Curie temperatures, from lava flows RA4, RA5, and RA6.

In conclusion, our extensive experiments are largely in agreement with previous studies concerning the sample selection criteria in that there should be an absence of viscosity and overprint and samples should have a single magnetic phase and be constituted mostly of single-domain grains. It seems also that samples having a high and narrow unblocking temperature spectrum are the best candidates for Thellier's experiment. This new criterium should be tested during future studies. However, even selected samples may not always give reliable results.

DISCUSSION

Geomagnetic field variations in direction and intensity recorded at sites A and B have been plotted on Figures 21a and 21b as a function of the volcanic stratigraphy. We can recognize that the site B has recorded less variations in direction as well as in intensity than flows from site A. Also, groups of flows

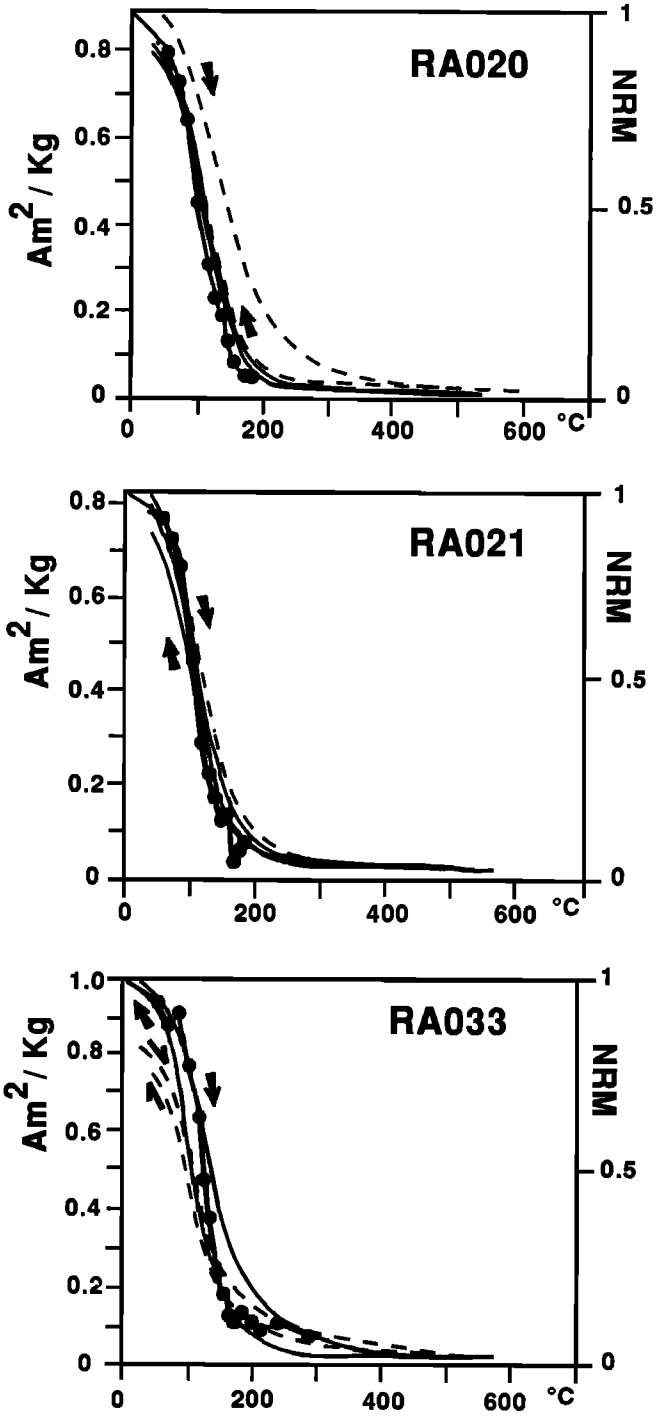

Fig. 20. Comparison of the NRM demagnetization (solid circles) with J_S-T experiments. Solid curves (dashed curves) correspond to Curie curves before (after) the paleointensity experiment. Very few variations in the Curie temperature are observed.

which have recorded very little variation in direction have provided similar paleointensity values within each group. For example, this is particularly clear for flows RB3, RB3bis, RB4 at section B, and RA1, RA2, and RA3 from section A. The major exceptions to this good relationship come from flows RB1-RB2 and RA13-RA15. Flow RB2 provides a mean paleointensity higher than the overlying flow RB1 which has the same paleomagnetic direction. This difference possibly does not correspond to true field variations but rather reflects problems in paleointensity determination because of the low-quality factors of the paleointensities from flow RB1 and the large scattering in the determinations available for flow RB2. The difference between flows RA13 and RA15 is also uncertain. Because several sources of uncertainties cannot be taken into account in the calculation of the error around the mean, we have chosen to plot the standard deviation calculated from two or three samples per flow and also an arbitrary error of about 30% of the mean flow paleointensity which would provide a better estimate of the confidence about the flow mean paleointensity. Extensive paleointensity determinations need to be done on historical lava flows for which the paleofield is known in order to better constrain the interpretation of paleointensity diagrams.

Comparison With the Present Day Field

Contrary to previous claims, it has recently been suggested that the secular variation of the present-day field is typical of that for the past 5 m.y. [*McFadden et al.*, 1988]. This result gives us confidence in the comparison between the present-day field at La Réunion and our paleomagnetic records. A sampling of the present day field on a parallel at about the latitude of La Réunion indicates variation in intensity from 24 to 53 μT. Assuming a westward drift of the nondipole sources of 0.2° per year, these intensities would be equivalent to a set of paleomagnetic data covering a period of 1800 years. The range of intensity variations of the present day field on this parallel is greater than that observed at site B but is of the same order as the one recorded at site A.

When significant directional changes occur between flows, paleointensities also vary as for example between lava flows RA3 and RA4 (Figure 21a). On the contrary, there is little evidence that the field intensity may vary without any change in direction.

In the Réunion records, a close examination of the relationships between directions and intensity of the field reveals that steepenings in inclination correspond to increases in intensity. This behavior is particularly clear on flows RA4-RA9. The present-day field also shows these features in the southern hemisphere with, for example low intensity and low inclination over South America and high inclination and high intensity over the Indian ocean.

A recent analysis of the magnetic field at the core mantle boundary (CMB) derived from observations since the beginning of the eighteen century has suggested that some features in the field have been stationary, while others appear at some fixed parts of the CMB before they drift westward [*Bloxham and Gubbins*, 1985]. Drifting features have been confined to the Atlantic hemisphere for the entire period, while low secular variation was observed in the Pacific hemisphere. Particularly, intense patches of reverse flux have been observed in the southern hemisphere around

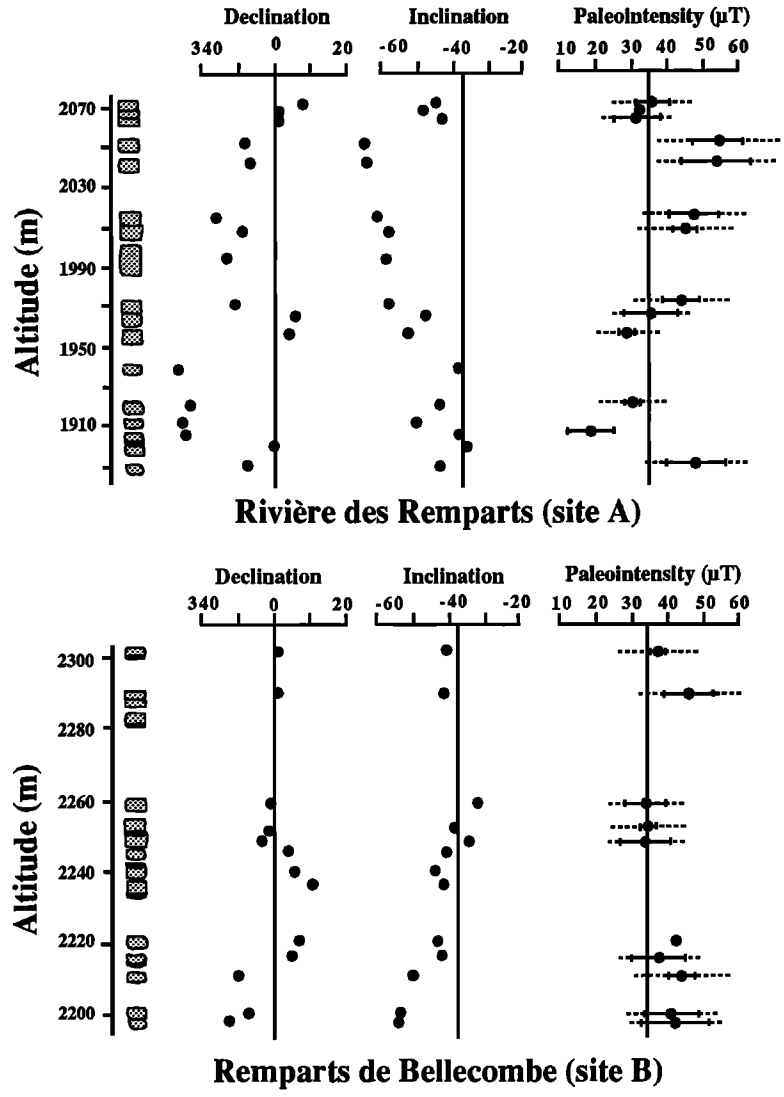

Fig. 21. For each sequence A and B, mean paleomagnetic directions and paleointensity results in μT (with one standard deviation) versus the stratigraphic height of each flow. Vertical lines refer to the inclination expected at this site for an axial dipole (-38°) and to the present-day field intensity (35 μT). The dashed lines associated to the flow mean paleointensity correspond to an error bar equal to 30% of the paleointensity.

90°E (South Africa) and are drifting westward toward South America. Both stationary and drifting features are interpreted to be associated with temperature anomalies in the lower mantle which may occur over the characteristic time scale of mantle convection [*Gubbins*, 1988]. The localization of these features at the CMB led *Gubbins* [1988] to predict some anomalies in the time-averaged magnetic field. For example, positive inclination anomalies (defined as the difference between the observed inclination and the one expected from a geocentric axial dipole) should exist for sites south of 45°S, while negative anomalies may be found at sites north of 30°S in the Atlantic hemisphere. The island of La Réunion is geographically well situated to test this model. Even though we may suspect that both flow sequences A and B did not completely average the secular variation, they both have negative inclination anomalies in support of Gubbin's predictions.

Comparison With Other Data From the Same Site

Paleointensity determinations, using both the Thellier and Shaw methods, were carried out by *Senanayake et al.* [1982], on volcanic rocks from the island of La Réunion. These lava flows which are significantly older (i.e., from 0.6 to 2 Ma.) provided field strengths from 19.4 to 40.2 μT. It indicates a range of variation similar to the one recorded on our late Quaternary sites.

Comparison With Worldwide Data

For the purpose of comparing our intensity data with those from sampling sites at different latitudes, it is convenient to calculate their equivalent virtual dipole moments (VDMs) which are reported in Table 2. In interpreting the results, we must keep in mind that

individual VDM values are composed by three factors: (1) the true dipole moment, (2) a portion due to nondipole components of the field which is unknown, and (3) errors in paleointensity determinations.

Global archaeomagnetic intensity data were analyzed by *Barton et al.* [1979], *Champion* [1980], and *McElhinny and Senanayake* [1982] using the largest data set. In order to average out nondipole field variations, results over 500- or 1000-year intervals have been averaged. The analysis of McElhinny and Senanayake shows that the mean dipole moment for the last 10,000-year interval is 8.75 $x10^{22}$ A m^2, a value very close to that obtained for the last 5 m.y., i.e., 8.7 $x10^{22}$ A m^2 [*McFadden and McElhinny*, 1982]. The average VDMs and standard deviation for the site B is 8.1 $\pm$0.7 $x10^{22}$ A m^2, a value in good agreement with the mean dipole moment for the last 10 kyr.

Most of the data corresponding to the time period 15-50 ka [*Barbetti and Flude*, 1979; *McElhinny and Senanayake*, 1982; *Salis*, 1987] tend to show that the geomagnetic field intensity was lower than the average value for the Holocene period. Several excursions of the field have also been reported in this period around 40–50 ka and low paleointensity values have been reported for the Laschamp excursion [*Roperch et al.*, 1988; *Marshall et al.*, 1988; *Chauvin et al.*, 1989]. There are no available data prior to 50 ka, and we may question whether the intensity low observed after the Laschamp excursion also occurred in the preceding period. VDMs obtained from the site A extend from 4.1 to 9.9 $x10^{22}$ A m^2 with a mean value and standard deviation around 7.3 $\pm$1.5 $x10^{22}$ A m^2, in good agreement with the mean value for the last 5 m.y. These data suggest variations with an amplitude about $\pm$50%, among which contributions from the dipole and the nondipole fields are not resolved. Because section A spans a time interval from 100 to 80 ka., the paleointensity results suggest that any dipole intensity low (if there is any) would not have lasted longer than 30 kyr prior to the Laschamp excursion and 20 kyr after the Blake excursion which occurred at 120 ka.

SUMMARY AND CONCLUSIONS

A detailed paleomagnetic study has been undertaken on two young volcanic sequences from the island of La Réunion; the oldest was built from 100 to 80 ka, while the youngest belongs to the Holocene period with age determinations from 11 to 5 ka.

The analysis of the geomagnetic secular variation of directions recorded by these sections indicates that the extrusion of the lava flows occurred by pulses separated by longer periods of quiescence. As a result of the extrusion process, the sampling of the paleomagnetic field was not complete enough to enable a statistically accurate determination of the mean field direction.

A detailed investigation of the magnetic properties of the samples was carried out, and numerous determinations of the paleointensity of the magnetic field have been attempted. A comparison of the low field susceptibility variations from liquid nitrogen temperature to room temperature with strong field thermomagnetic experiments confirms a previous study by *Senanayake and McElhinny* [1981] and indicates that low-temperature experiments provide a first-order approach to the magnetic composition of these basaltic rocks. This study emphasizes the need for selecting samples for paleointensity experiments. Samples very low in viscosity, with minimum secondary magnetization, rich in single-domain magnetic grains, and possessing one single well-defined magnetic phase and a high and narrow unblocking temperature distribution, are the best candidates for paleointensity experiments, even though these conditions may not insure reliable results.

Paleointensity estimates were obtained on 23 lava flows among the 30 which were sampled. For the youngest sequence, the VDMs do not depart much from the global mean dipole moment curve corresponding to the last 12 ka. This is interpreted as evidence of only minor nondipole sources at this site during that time.

For the other sequence, the VDMs variations are typical of nondipole field contributions superimposed on a mean VDM of possibly the same strength as the mean VDM for the past 10 kyr. This interpretation is supported by the paleomagnetic directions which also suggest contributions by nondipole terms.

Acknowledgments. Supporting reviews by D. Champion and R.S. Stenberg helped to improve this paper. A. Chauvin is grateful to P. Roperch for his help at all stages of this study. Financial support from INSU is acknowledged.

REFERENCES

Ade-Hall, J.M., H.C. Palmer, and T.P. Hubbard, The magnetic and opaque petrological response of basalts to regional hydrothermal alteration, *Geophys. J. R. astr. Soc.*, *24*, 137-174, 1971.

Aitken, M.J., P.A. Alcock, G.D. Bussell, and C.J. Shaw, Archaeomagnetic determination of the past geomagnetic intensity using ancient ceramics: Allowance for anisotropy, *Archaeometry*, *23* (1), 53-64, 1981.

Aitken, M.J., P.A. Alcock, G.D. Bussell, and C.J. Shaw Paleointensity studies on archaeological material from the near east, in *Geomagnetism of Baked Clays and Recent Sediments*, edited by K.M., Creer, P., Tucholka and, C.E. Barton, pp 122-127, Elsevier, New York, 1983.

Aitken, M.J., A.L. Allsop, G.D. Bussell, and M.B. Winter, Greek archeomagnitudes, *Nature*, *314*, 753, 1984.

Aitken, M.J., A.L. Allsop, G.D. Bussell, and M.B. Winter, Determination of the intensity of the Earth's magnetic field during archaeological times : Reliability of the Thellier technique, *Rev. Geophys*, *26* (1), 3-12, 1988.

Bachelery, P., Le Piton de la Fournaise (Ile de la Réunion) Etude volcanique, structurale et pétrologique, *Thèse de spécialité*, 215 pp., *Clermont-Ferrand*, 1981.

Barbetti, M.F., Archaeomagnetic results from Australia, in *Geomagnetism of Baked Clays and Recent Sediments*, edited by K.M., Creer, P., Tucholka and, C.E. Barton, pp 173-175, Elsevier, New York, 1983.

Barbetti, M.F., and K. Flude, Geomagnetic variation during the late Pleistocene period and changes in the radiocarbon time scale, *Nature*, *279*, 202-205, 1979.

Barton, C.E., R.T. Merrill, and M.F. Barbetti, Intensity of the Earth's magnetic field over the last 10 000 years, *Phys. Earth Planet. Inter.*, *20*, 96-110, 1979.

Bloxham, J., and D. Gubbins, The secular variation of the Earth's magnetic field, *Nature*, *317*, 777-781, 1985.

Bogue, S.W., and R.S. Coe, Transitional paleointensities from Kawaï, Hawaï and geomagnetic reversal models, *J. Geophys. Res.*, *89*, 10,341-10,354, 1984.

Burlatskaya, S.P., Archaeomagnetic investigations in the USSR, in *Geomagnetism of Baked Clays and Recent Sediments*, edited by K.M., Creer, P., Tucholka and, C.E. Barton, pp127-137, Elsevier, New York,1983.

Cassignol, P., and P.Y. Gillot, Range and effectiveness of unspiked potassium-argon dating: Experimental groundwork and applications, in: *Numerical Dating in Stratigraphy, edited by G.S. Odin, John Wiley, New York*, pp 159-179, 1982.

Chamalaun, F.H., Paleomagnetism of Réunion island and its bearing on secular variation, *J. Geophys. Res.*, *73*, 4647-4659, 1968.

Champion, D.E., Holocene geomagnetic secular variation in the western United States: Implications for the global Geomagnetic Field, *Ph.D. Thesis Pasadena, Calif.*, 1980.

Chauvin, A., R.A. Duncan, N. Bonhommet, and S. Levi, Paleointensity of the Earth's magnetic field and K-Ar dating of the Louchadière volcanic flow (central France). New evidence for the Laschamp excursion, *Geophys. Res. Lett.*, *16*, 1189-1192, 1989.

Cisowski, S.M., The relationship between the magnetic properties of terrestrial igneous rocks and the composition and internal structure of their components Fe oxide grains, *Geophys. J. R. astr. Soc.*, 60, 107-122, 1980.

Clark, D.A., and P.W. Schmidt Theoretical analysis of thermomagnetic properties, low-temperature hysteresis and domain structure of titanomagnetite, *Phys. Earth Planet. Inter.*, *30*, 300-316, 1982.

Coe, R.S., Poles-intensities of the Earth's magnetic field determined from Tertiary and Quaternary rocks, *J. Geophys. Res.*, *72*, 3247-3262, 1967a.

Coe, R.S., Determination of paleo-intensities of the Earth's magnetic field with emphasis on mechanisms which could cause non-ideal behavior in Thellier's method, *J. Geomagn. Geoelectr.*, *19*, 157-179, 1967b.

Coe, R.S., and S. Gromme, A comparison of three methods of determining geomagnetic paleointensities, *J. Geomag. Geoelec.*, *25*, 415-435, 1973.

Coe, R.S., S. Gromme, and E.A. Mankinen, Geomagnetic paleointensities from radiocarbon dated lava flows on Hawaï and the question of the Pacific non-dipole low, *J. Geophys. Res.*, *83*, 1740-1756, 1978.

Coe, R.S., S. Gromme, and E.A. Mankinen, Geomagnetic paleointensities from excursion sequences in lavas on Oahu, Hawaï, *J. Geophys. Res.*, *89*, 1059-1069, 1984.

Cox, A., Research note: Confidence limits for the precision parameter *k*, *Geophys. J. R. astr. Soc.*, *18*, 545-549, 1969.

Day, R., M. Fuller, and V.A. Schmidt, Hysteresis properties of titanomagnetites: Grain size and compositional dependance, *Phys. Earth Planet. Inter.*, *13*, 260-267, 1977.

Dodson, M.H., and E. McClelland-Brown, Magnetic blocking temperatures of single domain grains during slow cooling, *J. Geophys. Res.*, *85*, 2625-2637, 1980.

Duffield, W.A., L. Stieltjes, and J. Varet, Huge landslide blocks in the growth of Piton de la Fournaise, la Réunion and Kilauea volcano, Hawaii, *J. Volcanol. Geotherm. Res.*, *12*, 147-160, 1982.

Dunlop, D.J., Thermal enhancement of magnetic susceptibility, *J. Geophys.*, *40*, 439-451, 1974.

Dunlop, D.J., The rock magnetism of fine particles, *Phys. Earth Planet. Inter.*, *26*, 1-26, 1981.

Dunlop, D.J., Determination of domain structure in igneous rocks by alternating field and other methods, *Earth Planet. Sci. Lett*, *63*, 353-367, 1983.

Emerick, C.M., and R.A. Duncan, Age progressive volcanism in the Comores archipelago, Western Indian Ocean and implications for Somali plate tectonics, *Earth Planet. Sci. Lett.*, *60*, 415-428, 1982.

Fox, J.M.W., and M.J. Aitken, Cooling rate dependence of thermoremanent magnetization, *Nature*, *283*, 462-463, 1980.

Games, K.P., The magnitude of the archaeomagnetic field in Egypt between 3000 and 0 BC, *Geophys. J. R. astr. Soc.*, *63*, 45-56, 1980.

Games, K.P., Archaeomagnitude results from Egypt, in *Geomagnetism of Baked Clays and Recent Sediments*, edited by K.M., Creer, P., Tucholka and, C.E. Barton, pp 111-116, Elsevier, New York, 1983a.

Games, K.P., Results from Peru, in *Geomagnetism of Baked Clays and Recent Sediments*, edited by K.M., Creer, P., Tucholka and, C.E. Barton, pp 167-172, Elsevier, 1983b.

Gillot, P.Y., and P. Nativel, K-Ar chronology of the ultimate activity of Piton des Neiges volcano, Réunion Iceland, Indian Ocean, *J. Volcanol Geotherm. Res.*, *13*, 131-146, 1982.

Gillot, P.Y., and P. Nativel, Eruptive history of the Piton de la Fournaise volcano, Reunion island, Indian Ocean, *J. Volcanol Geotherm. Res.*, *36*, 53-65, 1989.

Gromme, C.S., T.L. Wright, and D.L. Peck, Magnetic properties and oxidation of iron-titanium oxide minerals in Alae and Makaopuhi lava lakes, Hawaï, *J. Geophys. Res.*, *74*, 5277-5293, 1969.

Gromme, S., E.A. Mankinen, M. Marshall, and R.S. Coe, Geomagnetic paleointensities by the Thellier's method submarine pillow basalts, effects of seafloor weathering, *J. Geophys. Res.*, *84*, 3553-3575, 1979.

Gubbins, D., Thermal core-mantle interaction and time-averaged paleomagnetic field, *J. Geophys. Res.*, *93*, 3413-3420, 1988.

Halgedahl, S.L., R. Day, and M. Fuller, The effect of cooling rate on the intensity of weak field TRM in single domain magnetite, *J. Geophys. Res.*, *85*, 3690-3698, 1980.

Hirooka, K., Results from Japan, in *Geomagnetism of Baked Clays and Recent Sediments*, edited by K.M., Creer, P., Tucholka and, C.E. Barton, pp 150-157, Elsevier, New York, 1983.

Khodair, A.A., and R.S. Coe Determination of geomagnetic paleointensities in vacuum, *Geophys. J. R. astr. Soc.*, *42*, 107-115, 1975.

King, J.W., S.K., Banerjee, and J. Marvin, A new rock-magnetic approach to selecting sediments for geomagnetic paleointensity studies: Application to paleointensity for the last 40000 years, *J. Geophys. Res.*, *88*, 5911-5921, 1983.

Kono, M., Changes in TRM and ARM in a basalt due to laboratory heating, *Phys. Earth Planet. Inert.*, *46*, 1-19, 1987.

Kono, M., and N. Ueno, Paleointensity determination by a modified Thellier method, *Phys. Earth Planet. Inter.*, *13*, 305-314, 1977.

Kono, M., and H.Tanaka, Analysis of the Thellier's method of paleointensity determination 1 : Estimation of statistical errors, *J. Geomagn. Geoelectr.*, *36*, 267-284, 1984.

Kono, M., N. Ueno, and Y. Onuki, Paleointensities of the geomagnetic field obtained form Pre-Inca potsherds, near Cajamarca: Northern Peru, *J. Geomag. Geoelectr.*, *38*, 1339-1348, 1986.

Kovacheva, M., Summarized results of the archaeomagnetic investigation of the geomagnetic field variation for the last 8 000 yr in South-Eastern Europe, *Geophys. J. R. astr. Soc.*, *61*, 57-64, 1980.

Kovacheva, M., Archaeomagnetic investigations of geomagnetic secular variations, *Philos. Trans. R. Soc. London*,.ser A, *306*, 79-86, 1982.

Kovacheva, M., Existing archeointensity data from Bulgaria and South Eastern Yugoslavia. in *Geomagnetism of Baked Clays and Recent Sediments*, edited by K.M., Creer, P., Tucholka and, C.E. Barton, pp 106-110, Elsevier, New York, 1983.

Levi, S., Comparison of two methods of performing the Thellier experiment (or, how the Thellier method should not be done), *J. Geomag. Geoelectr.*, *27*, 245-255, 1975.

Levi, S., The effect of magnetite particle size on paleointensity determinations of the geomagnetic field, *Phys. Earth Planet. Inter.*, *13*, 245-259, 1977.

Levi, S., The additivity of partial thermal remanent magnetization in magnetite, *Geophys. J. R. astr. Soc.*, *59*, 205-218, 1979.

Levi, S., and S.K. Banerjee, On the possibility of obtaining relative paleointensities from Lake sediments, *Earth. Planet. Sci. Lett.*, *29*, 219-2226, 1976.

Levi, S., and R.T. Merrill, Properties of single-domain, pseudo-single-domain and multidomain magnetite, *J. Geophys. Res.*, *83*, 245-259, 1977.

Lowrie, W., and M. Fuller, On the alternating field demagnetization characteristics of multidomain thermoremanent magnetization in magnetite, *J. Geophys. Res.*, *76*, 6339-6349, 1971.

Mankinen, E.A, M. Prévot, G.S. Gromme, and R.S. Coe, The Steen's Mountain (Oregon) geomagnetic polarity transition 1. Directional history, duration of episodes, and rocks magnetism, *J. Geophys. Res.*, *90*, 10,393-10,416, 1985.

Marshall, M., A. Chauvin, and N. Bonhommet, Preliminary paleointensity measurements and detailed magnetic analysis of basalts from the Skalamaelifell excursion, southwest Iceland, *J. Geophys. Res.*, *93*, 11,681-11,698, 1988.

McClelland-Brown, E., Experiments on TRM intensity dependence on cooling rate, *Geophys. Res. Lett.*, *11*, 205-208, 1984.

McDougall, I., The geochronology and evolution of the young volcanic island of Réunion, Indian Ocean, *Geochim. Cosmochim. Acta*, *35*, 261-288, 1971.

McElhinny, M.W., and W.E. Senanayake, Variations in the geomagnetic dipole. 1 The past 50,000 years, *J. Geomagn. Geoelectr.*, *34*, 39-51, 1982.

McFadden, P.L., and M.W. McElhinny, Variations in the geomagnetic dipole. 2 Statistical analysis of VDMs for the past 5 millions years, *J. Geomagn. Geoelectr.*, *34*, 163-189, 1982.

McFadden, P.L., and R.T. Merrill, A physical model for palaeosecular variation, *Geophys. J. R. astr. Soc.*, *78*, 809-830, 1984.

McFadden, P.L., R.T. Merrill, and M.W. McElhinny, Dipole/quadrupole family of paleosecular variation, *J. Geophys. Res.*, *93*, 11,583-11,588, 1988.

Merrill R.T., and M.W. McElhinny, The Earth's Magnetic Field, Its History, Origin and Planetary Perspective, *Int. Geophys. Ser.*, vol: 32, *Academic Press*, 1983.

Moskowitz, B.M., Methods for estimating Curie temperature of titanomagnetites from experimental Js-T data, *Earth Planet. Sci. Lett.*, *53*, 84-88, 1981.

Prévot, M., Magnétisme et minéralogie magnétique de roches néogènes et quaternaires, contribution au paléomagnétisme et à la géologie du Velay, *Thèse, Univ. P. et M. Curie*, Paris, 1975.

Prévot, M., E.A. Mankinen, and S. Gromme, High paleointensities of the Geomagnetic field from thermomagnetic studies on rift valley pillow basalts from the Mid-Atlantic Ridge, *J. Geophys. Res.*, *88*, 2316-2326, 1983.

Prévot, M., E.A. Mankinen, R.S. Coe, and C.S. Gromme, The Steens Mountain geomagnetic polarity transition, 2 Field intensity variation and discussion of reversal models, *J. Geophys. Res.*, *90*, 10,417-10,448, 1985.

Radhakrishnamurty, C., and E.R. Deutsch, Magnetic techniques for ascertaining the nature of iron oxide grains in basalts, *J. Geophys.*, *40*, 453-465, 1974.

Radhakrishnamurty, C., E.R. Deutsch, and G.S. Murthy, On the presence of titanomagnetite in basalts, *J. Geophys.*, *45*, 433-446, 1979.

Ramaswamy, K., M. Dheenathayalu, and S. Bharathan, Archaeomagnetic determination of the ancient intensity of the geomagnetic field in Tamilnadu, India, *Phys. Earth Plan. Inter.*, *40*, 61-64, 1985.

Readman, P.L., and W. O'Reilly, Magnetic properties of oxidized (cation-deficient) titanomagnetite (Fe, Ti)$_3$ O$_4$, *J. Geomagn. Geoelectr.*, *24*, 69-90, 1972.

Roperch, P., N. Bonhommet, and S. Levi, Paleointensity of the Earth's magnetic field during the Laschamp excursion and geomagnetic implications, *Earth Planet. Sci. Lett.*, *88*, 209-219, 1988.

Salis, J.S., Variation séculaire du champ magnétique terrestre. Directions et paleointensités - sur la période 7000-70 000 ans BP, dans la Chaîne des Puys, *Thèse Univ. Rennes, Mémoires et documents du CAESS*, *11*, France, 1987.

Salis, J.S, N. Bonhommet and S. Levi, Paleointensity of the geomagnetic field from dated lavas of the Chaîne des Puys, France, 1, 7-12 thousand years before present, *J. Geophys. Res.*, *94*, 15,771-15,784, 1989.

Schweitzer, C., and H.C. Soffel, Paleointensity measurements on post glacial lavas from Iceland, *J. Geophys.*, 47, 57-60, 1980.

Senanayake, W.E., and M.W. McElhinny, Hysteresis and susceptibility characteristics of magnetite and titanomagnetites: Interpretation of results from basaltic rocks, *Phys. Earth Planet. Inter.*, *26*, 47-55, 1981.

Senanayake, W.E., and M.W. McElhinny, The effects of heating on low temperature susceptibility and hysteresis properties of basalts, *Phys. Earth. Planet. Inter.*, *30*, 317-321, 1982.

Senanayake, W.E., M.W. McElhinny, and P.L. Mc McFadden, Comparison between the Thellier's and Shaw's paleointensity methods using basalts less than 5 million years old, *J. Geomagn. Geoelectr.*, *34*, 141-161, 1982.

Soffel, H., The single domain-multidomain transition in natural intermediate titanomagnetites, *J. Geophys.*, *37*, 451-470, 1971.

Sternberg, R.S., Archaeomagnetism in the Southwest of North America, in *Geomagnetism of Baked Clays and Recent Sediments*, edited by K.M., Creer, P., Tucholka and, C.E. Barton, pp 158-167, Elsevier, New York, 1983.

Sternberg, R.S., Archaeomagnetic paleointensity in the American southwest during the past 2000 years, *Phys. Earth Planet. Inter.*, *56*, 1-17, 1989.

Sternberg, R.S., and R.F. Butler, An archaeomagnetic paleointensity study of some Hohokan potsherds from Snaketown, Arizona, *Geophys. Res. Lett.*, *5*, 101-104, 1978.

Tanaka, H., Intensity variation of the geomagnetic field in Japan during the last 30,000 years, determined from volcanic rocks and potteries. *Ph.D. thesis, Tokyo Inst. Tech.*, 1980.

Tanaka, H., and M., Kono, Analysis of the Thellier's method of paleointensity determination, 2: Application to high and low magnetic fields, *J. Geomagn. Geoelectr.*, *36*, 285-297, 1984

Thellier, E., and O. Thellier, Recherches géomagnétiques sur

des coulées volcaniques d'Auvergne, *Ann. Geophys.*, *1*, 37-42, 1944.

Thellier, E., and O. Thellier, Sur l'intensité du champ magnétique terrestre dans le passé historique et géologique, *Ann. Geophys.*, *15*, 285-376, 1959.

Walton, D., Geomagnetic intensity in Athens between 2,000 BC and AD 400, *Nature*, *277*, 643-644, 1979.

Walton, D., Re-evalution of Greek archaeomagnitudes, *Nature*, *310*, 740-743, 1984.

Watkins, N.D., Brunhes epoch geomagnetic secular variation on Réunion Island, *J. Geophys. Res.*, *78*, 7763-7768, 1973.

Watkins, N.D., and J. Nougier, Excursions and secular variation of the Brunhes Epoch. Geomagnetic field in the Indian Ocean region, *J. Geophys. Res.*, *78*, 6060-6068, 1973.

Wei, Q.Y., Z. Wei-Xi , L. Dong-Jie, M. J. Aitken, G.D. Bussell, and M. Winter, Geomagnetic intensities as evaluated from ancient Chinese pottery, *Nature*, *328*, 330-333, 1987.

Worm, H.L., M. Jackson, P. Kelso, and S.K. Banerjee, Thermal demagnetization of partial thermoremanent magnetization, *J. Geophys. Res.*, *93*, 12,196-12,204, 1988.

York, D., Least-squares fitting of a straight line, *Can. J. Phys.*, *44*, 1079-1086, 1966.

York, D., The best isochron, *Earth Planet. Sci. Lett.*, *2*, 479-482, 1967.

N. Bonhommet, Département de Géotectonique, Université de Paris VI, 75252 Paris Cedex 05, France.

A. Chauvin, Laboratoire de Géophysique Interne, CAESS, Université de Rennes I, 35042 Rennes Cedex, France.

P.-Y. Gillot, Centre des Faibles Radioactivités, CEA-CNRS, Av. de la Terrasse, 91190 Gif sur Yvette, France

(Received April 18, 1989;
revised September 28, 1990;
accepted September 28, 1990)